Gibco) supplemented with 10% FCS and $5 \times 10^{-2}$ μM 2ME and without LIF. After 5 days, the induced cells were treated with 0.25% trypsin/EDTA, and $1.2 \times 10^4$ total cells/cm$^2$ or $1.2 \times 10^3$ sorted Flk-1$^+$ cells/cm$^2$ were transferred onto fresh semi-confluent OP9 cell layers, and cultured thereafter for hematopoietic differentiation in α-MEM supplemented with 10% FCS, $5 \times 10^{-2}$ μM 2ME, and the following four recombinant growth factors: 100 ng/ml mouse stem-cell factor (mSCF), 4 ng/ml human thrombopoietin (hTPO), 20 ng/ml mouse interleukin 3 (mIL3), and 2 U/ml human erythropoietin (hEPO). These cytokines were kindly provided by Kirin Brewery (Tokyo, Japan).

### RNA extraction and RT-PCR analysis

RNA samples were prepared using silica gel membrane-based spin-columns (RNeasy Mini-Kit™; Qiagen, Valencia, CA) and subjected to RT with a Sensiscript-RT Kit™ (Qiagen). All procedures were performed following the manufacturer's instructions. For RT-PCR, yields were adjusted by dilution to produce equal amounts of the glyceraldehyde-3-phosphate dehydrogenase (GAPDH) amplicon. Complementary DNA (cDNA) templates were initially denatured at 94°C for 5 min, followed by 29–35 amplification reactions consisting of 94°C for 15 sec (denaturing), 55–64°C for 15 sec (annealing), and 72°C for 30 sec (extension), with a final extension at 94°C for 7 min. The oligonucleotide primers were as follows: *GAPDH*, 5′-TCC AGA GGG GCC ATC CAC AGT C-3′ and 5′-GTC GGT GTG AAC GGA TTT GGC C-3′ (Baba et al., 2007a); *Rex1*, 5′-AAA GTG AGA TTA GCC CCG AG-3′ and 5′-TCC CAT CCC CTT CAA TAG CA-3′ (Baba et al., 2007a); *Brachyury*, 5′-CAT GTA CTC TTT CTT GCT GG-3′ and 5′-GGT CTC GGG AAA GCA GTG GC-3′ (Ku et al., 2004); *Flk-1*, 5′-CAC CTG GCA CTC TCC ACC TTC-3′ and 5′-GAT TTC ATC CCA CTA CCG AAA G-3′ (Baba et al., 2007a); *Scl*, 5′-ATG GAG ATT TCT GAT GGT CCT CAC-3′ and 5′-AAG TGT GCT TGG GTG TTG GCT C-3′ (Baba et al., 2007a); *Myb*, 5′-CAC CAT TCT GGA CAA TGT TAA GAA C-3′ and 5′-GTA AGG TAG GTG CAT CTA AGC-3′; *Tie1*, 5′-ATA CCC TAG ACT GGC AAG AG-3′ and 5′-TTT TGA CAC TGG CAC TGG A-3′; *Gata1*, 5′-GCT GAA TCC TCT GCA TCA AC-3′ and 5′-TAG GCC TCA GCT TCT CTG TA-3′ (Shimizu et al., 2001); *Gata2*, 5′-GCA ACA CAC CAC CCG ATA CC-3′ and 5′-CAA TTT GCA CAA CAG GTG CCC-3′ (Shimizu et al., 2004); *ε-globin*, 5′-GGA GAG TCC ATT AAG AAC CTA GAC AA-3′ and 5′-CTG TGA ATT CAT TGC CGA AGT GAC-3′ (Hansen et al., 1982); *ζ-globin*, 5′-GCT CAG GCC GAG CCC ATT GG-3′ and 5′-TAG CGG TAC TTC TCA GTC AG-3′ (Leder et al., 1985); *α-globin*, 5′-CTC TCT GGG GAA GAC AAA AGC AAC-3′ and 5′-GGT GGC TAG CCA AGG TCA CCA GCA-3′ (Nishioka and Leder, 1979); *β-globin*, 5′-CTG ACA GAT GCT CTC TTG GG-3′ and 5′-CAC AAC CCC AGA AAC AGA CA-3′ (Konkel et al., 1978); *Oct3/4* (Tg), 5′-AAA AAG CAG GCT CCA CCT TCC CCA TGG CTG GAC ACC-3′ and 5′-AGA AAG CTG GGT TGA TCA ACA GCA TCA CTG AGC TTC-3′ (Takahashi and Yamanaka, 2006); *Sox2* (Tg), 5′-AAA AAG CAG GCT TGT ATA ACA TGA TGG AGA CGG-3′ and 5′-AGA AAG CTG GGT TTC ACA TGT GCG ACA GGG GCA GT-3′ (Takahashi and Yamanaka, 2006); *c-Myc* (Tg), 5′-CAC CAT GCC CCT CAA CGT GAA CTT CAC C-3′ and 5′-TTA TGC ACC AGA GTT TCG AAG CTG TTC G-3′ (Takahashi and Yamanaka, 2006); *Klf4* (Tg), 5′-CAC CAT GGC TGT CAG CGA CGC TCT GCT C-3′ and 5′-ACA TCC ACT ACG TGG GAT TTA AAA-3′ (Takahashi and Yamanaka, 2006).

### Real-time quantitative RT-PCR analysis

Forward and reverse primers for *Rex1* and *Flk-1* and the fluorogenic probes were designed according to PerkinElmer guidelines (Primer Express Software; PerkinElmer Life and Analytical Sciences, Boston, MA, http://www.perkinelmer.com), and those of *Brachyury* and *Scl* were described in a previous report (Nakanishi et al., 2009; Redmond et al., 2008). The *GAPDH* primers and probes were purchased from Applied Biosystems (Foster City, CA, http://www.appliedbiosystems.com). Quantitative RT-PCR experiments were performed using the ABI-Prism 7300 system (Applied Biosystems) following the manufacturer's instructions. Quantitative assessment of mRNA expression was performed using a GAPDH internal standard. The expression of each mRNA was compared with each day 0 mRNA expression.

The oligonucleotide primers were as follows: mouse *Rex1*, 5′-AAG CAG GAT CGC CTC ACT GT-3′ and 5′-CCG CAA AAA ACT GAT TCT TGG T-3′ (Baba et al., 2007a); mouse *Brachyury*, 5′-TAC CCC AGC CCC TAT GCT CA-3′ and 5′-GGC ACT CCG AGG CTA GAC CA-3′ (Nakanishi et al., 2009); mouse *Scl*, 5′-CAC TAG GCA GTG GGT TCT TTG-3′ and 5′-GGT GTG AGG ACC ATC AGA AAT CT-3′ (Redmond et al., 2008); mouse Flk-1, 5′-AAG CAG GAT CGC CTC ACT GT-3′ and 5′-CCG CAA AAA ACT GAT TCT TGG T-3′ (Baba et al., 2007a).

### Colony-forming assay

Every other day of culture, from days 5 through 15, the adherent cells were treated with 0.25% trypsin/EDTA and harvested. They were incubated in a new tissue-culture dish (Becton–Dickinson) for 30 min to eliminate adherent OP9 cells (Suwabe et al., 1998). Floating cells were then collected and cultured at a concentration of $1 \times 10^4$ cells/ml in semi-solid α-MEM supplemented with 1.3% methylcellulose, 30% FCS, 10% bovine serum albumin, 100 μM 2ME, and a mixture of the following growth factors: 10 ng/ml human granulocyte colony-stimulating factor (hG-CSF), 2 U/ml hEPO, 20 ng/ml mIL3, 100 ng/ml mSCF, 100 ng/ml hIL6, and 10 ng/ml hTPO. Colony types were determined according to the criteria described previously (Nakahata and Ogawa, 1982a,b,c) by in situ observation using an inverted microscope. The abbreviations used for the clonogenic progenitor cells were as follows: CFU-Mix, mixed colony-forming units; BFU-E, erythroid burst-forming units; CFU-GM, granulocyte–macrophage colony-forming units; and CFU-G, granulocyte colony-forming units.

### Single-cell deposition assay

The single-cell deposition assay was performed as described previously (Nishikawa et al., 1998; Umeda et al., 2006; Shinoda et al., 2007). In brief, single sorted cells were deposited in individual wells of 96-well plates with confluent OP9 layers, and cultured for 5 days in the medium described in the "Differentiation of iPS and ES Cells" Section. Each well was stained with a mixture of anti-CD45, CD41, and Ter119 rat antibodies for hematopoietic lineage detection or anti-VE-cadherin rat-antibodies for endothelial lineage detection, respectively. HRP-conjugated goat anti-rat antibodies (Jackson ImmunoResearch Laboratories, Inc.) were used as secondary antibodies.

### Statistics

Statistical analyses were conducted using the Student's *t*-test or the Fisher's exact test. Statistical significance was defined as $P < 0.05$.

## Results

### iPS cells differentiate into hematopoietic cells in coculture with OP9 stromal cells

We initially compared iPS and ES cells by microscopic examination and FACS analysis. The Nanog-iPS cell lines (Okita

et al., 2007) (20D17, 38C2, and 38D2) were positive for green fluorescent protein (GFP) expression only when Nanog was activated. 256H18, which was established by introducing only Oct3/4, Sox2, and Klf4, expressed DsRed (Nakagawa et al., 2008) constitutively. The pMx-GFP retrovirus was introduced into this clone as a silencing indicator. The control D3 ES cells were constitutively positive for GFP. All four of the iPS clones formed ES-like colonies over more than 15 passages (Fig. 1A). The FACS analysis revealed that all of the clones expressed SSEA1, E-cadherin, and CD31 (Fig. 1B), thus demonstrating the phenotypic similarity between iPS and ES cells.

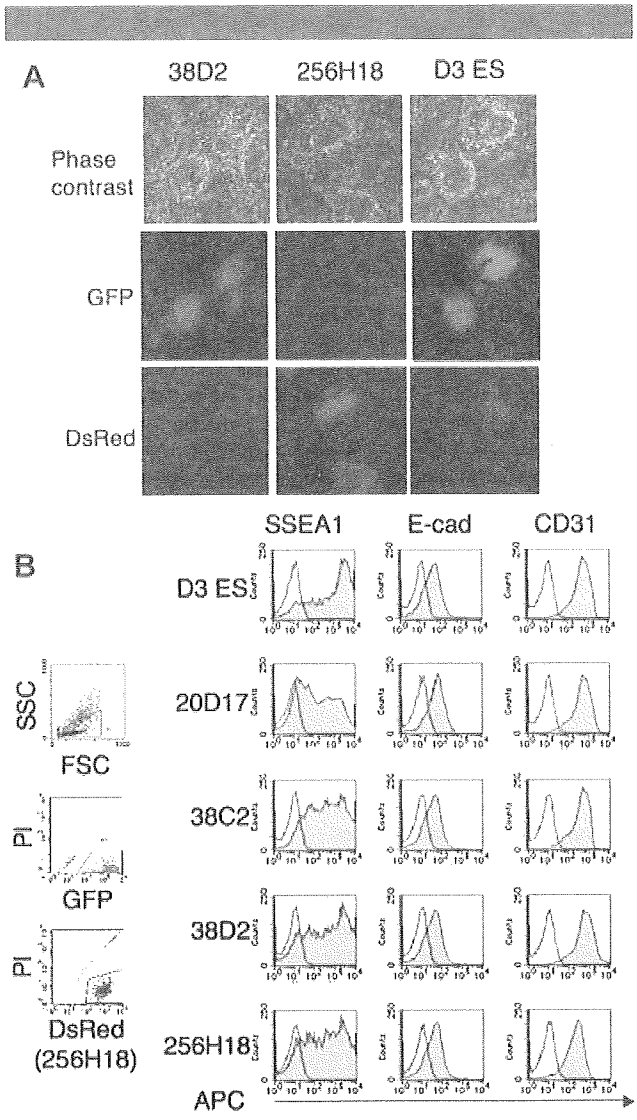


Fig. 1. Formation of ES-like colonies from iPS cells. A: Phase contrast (top row) and fluorescence (middle row: GFP, bottom row: DsRed) micrographs of Nanog-iPS cells (38D2), three-factor (without Myc) iPS (256H18) cells, and D3 ES cells maintained on SNL feeder cells. The D3 ES cells were derived from GFP$^+$ mice. Nanog-iPS cells express GFP only in the undifferentiated state. The three-factor iPS cells were derived from DsRed$^+$ mice, with additional infection by the pMx-GFP virus as a silencing marker. B: FACS analysis showing the phenotypic similarity of iPS and ES cells. The left parts show the gates for eliminating dead cells and contaminated feeders. GFP$^+$PI$^-$ cells (R2) and DSRed$^+$PI$^-$ cells (R4) were gated as ES- and iPS-derived viable cells, respectively. SSEA1, E-cadherin, and CD31 were positive in all strains (shaded bars). Open bars show staining with isotype control antibodies. Representative results from one of three independent experiments performed are presented.

To analyze the hematopoietic differentiation potential of iPS cells, we adapted the OP9 coculture system originally reported by Nakano et al. (1994, 1996). We cocultured iPS cells with OP9 stromal cells for 5 days and transferred the entire culture onto fresh OP9 layers in the presence of mSCF, mIL3, hTPO, and hEPO. Small, round cell colonies first appeared 2 days later (on day 7; Fig. 2A). These colonies gradually grew in both size and number, and a few exhibited areas with a cobblestone-like appearance. Floating cells also appeared on day 7 and thereafter. May–Giemsa staining of the floating cells on day 15 revealed enucleated red blood cells, macrophages, granulocytes, and megakaryocytes (Fig. 2B). The presence of granulocytes and megakaryocytes was confirmed by MPO and acetylcholine esterase (Maherali et al., 2007) staining, respectively. FACS analysis on day 15 confirmed the existence of various types of blood cells, including erythoid and myeloid lineage cells, but not of lymphoid lineage cells (Fig. 2C). These above results demonstrate that iPS cells, like ES cells, can produce hematopoietic cells of various lineages in vitro.

### Efficient production of hematopoietic cells from sorted Flk-1$^+$ cells

To thoroughly investigate iPS cell-derived hematopoietic development, we analyzed the expression of Flk-1, a marker of hemoangiogenic progenitors. Although the proportion of Flk-1$^+$ cells in the iPS clones on day 5 varied between 20 ± 2% and 48 ± 9% (Fig. 3A), the temporal patterns of expression were similar in iPS and ES cells. No Flk-1$^+$ cells were detected at

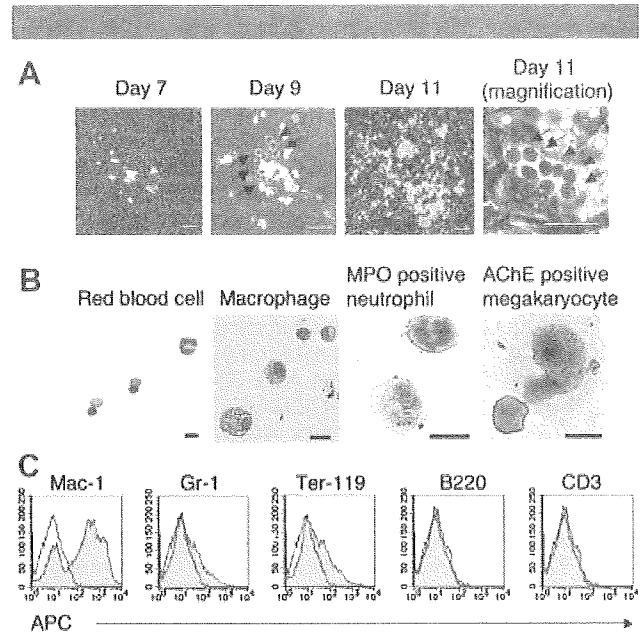


Fig. 2. Hematopoietic cells develop from iPS cells on OP9 feeders. Data from clone 38D2 are shown as representative of iPS-derived hematopoiesis. A: Small colonies first appeared on day 7 (2 days after Flk1$^+$ sorting) and then grew larger. Dark, round hematopoietic progenitors (indicated by arrows) appeared on days 9 and 11, lying beneath the OP9 layer and presenting cobblestone-like areas. Scale bars, 200 μm (left three parts) and 100 μm (rightmost part). B: Floating cells on day 15 included various lineages of hematopoietic cells; enucleated red blood cells, macrophages, MPO$^+$ neutrophils, and AChE$^+$ megakaryocytes were observed. Scale bars, 50 μm. C: Expression of lineage-specific antigens. Floating cells on day 15 were stained with antibodies against macrophages (Mac-1), granulocytes (Gr-1), erythrocytes (Ter-119), B cells (B220), and T cells (CD3). Expression of each antigen (shaded bars) was analyzed using FACS. Open bars show staining with isotype control antibodies.

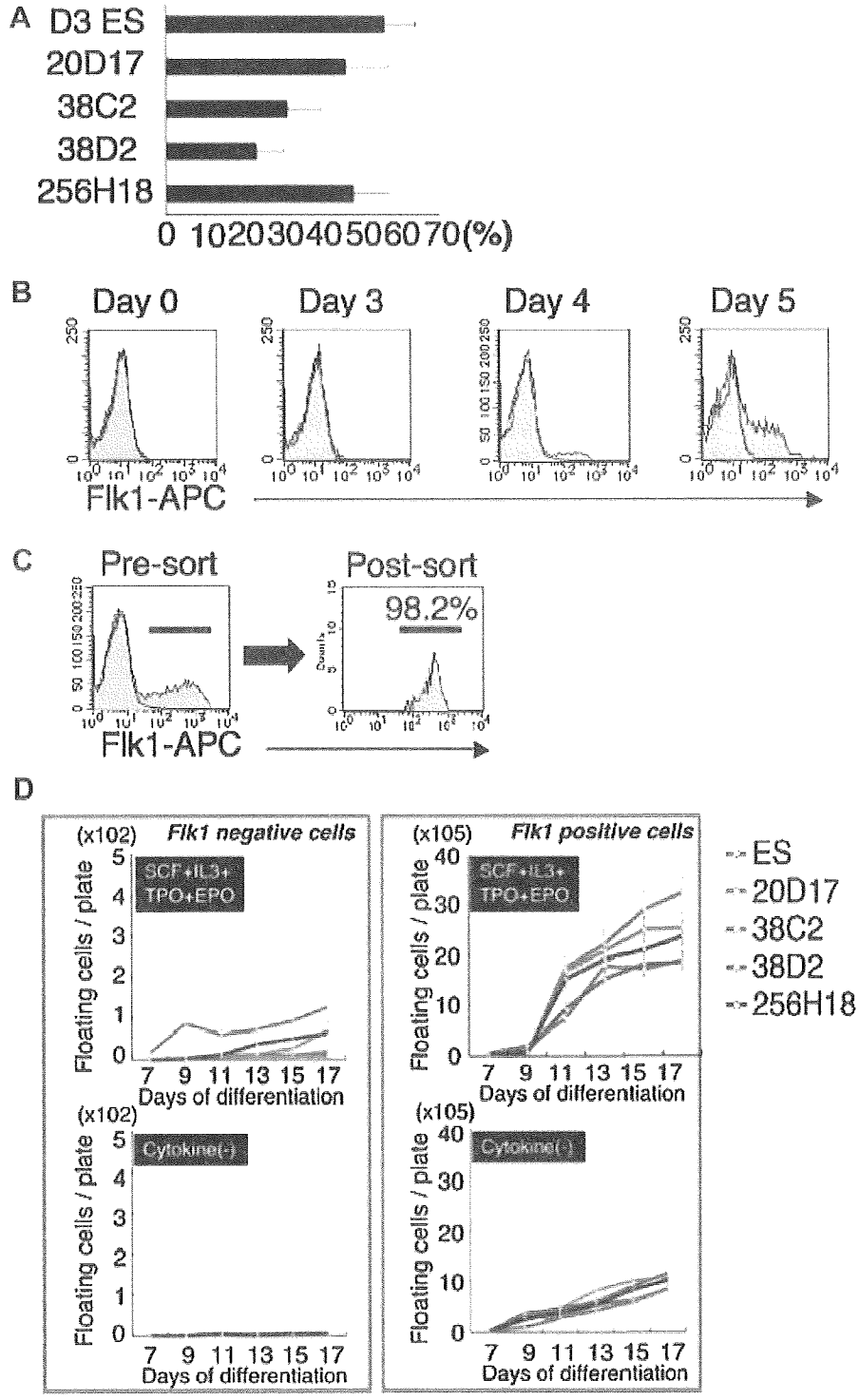


Fig. 3. Efficient production of hematopoietic cells from Flk-1$^+$ populations. A: The amounts of Flk-1$^+$ cells generated from ES and iPS cells at day 5 of differentiation were analyzed by FACS after eliminating OP9 stromal cells as described in Materials and Methods Section. Data are shown as a percentage in the total ES- and iPS-derived viable cells. B: Sequential FACS analysis reveals the emergence of Flk-1$^+$ population after day 4 of differentiation (shaded bars). Open bars show staining with isotype control antibodies. C: Purification of Flk-1$^+$ fractions by FACS on day 5. Reanalysis of the sorted cells confirmed the purity as 93.0–98.2%. D: Sequential analysis of the number of floating cells from ES and iPS cells after sorting with Flk-1 antibody. Sorted Flk-1$^+$ and Flk-1$^-$ cells were cultured in the presence or absence of SCF, IL-3, TPO, and EPO. In (A) and (D), data are presented as mean ± SE of three independent duplicate experiments. In (B) and (C), representative data from clone 38D2 are shown.

the outset, but they appeared on day 4 of culture and increased in number until day 5 (Fig. 3B).

We next sorted the Flk-1$^+$ cells on day 5 and cocultured them with fresh OP9 cells. Reanalysis of the sorted Flk-1$^+$ cells by FACS showed that their purity ranged from 93.0% to 98.2% (Fig. 3C). Regardless of the percentage of Flk1$^+$ cells before sorting, all of the iPS cell lines and ES cells could produce similar yields of hematopoietic cells predominantly from Flk-1$^+$ fractions, and exogenous cytokines increased the hematopoietic efficacy fourfold (Fig. 3D).

### Primitive and definitive hematopoietic development of iPS cells

In the developing mouse embryo, primitive hematopoiesis originates in the extra-embryonic yolk sac on day 7.5 of gestation (Moore and Metcalf, 1970). Thereafter, definitive hematopoiesis emerges as a second wave in the aorta-gonad-mesonephros (AGM) region and replaces primitive hematopoiesis (Muller et al., 1994; Medvinsky and Dzierzak, 1996; Matsuoka et al., 2001). Primitive and definitive erythrocytes are morphologically distinguishable, and show distinct patterns of hemoglobin gene expression: the former are larger, nucleated cells that express not only embryonic ε-globin and ζ-globin but also adult α-globin, whereas the latter are smaller, enucleated cells expressing only adult α-globin and β-globin (Doetschman et al., 1985; Leder et al., 1992; Nakano et al., 1996; Xu et al., 2001).

To investigate whether primitive and definitive erythropoiesis can occur in iPS cells, we initially examined floating hematopoietic cells (Fig. 4A). May–Giemsa staining revealed that on day 7 the cells were large and nucleated, resembling primitive erythrocytes, whereas on day 15 they were smaller, enucleating or enucleated, and similar to definitive erythrocytes. Immunostaining revealed that day 7 cells were strongly positive for embryonic hemoglobin but negative for β-major hemoglobin, while day 15 cells expressed β-major hemoglobin strongly, with little or no expression of embryonic hemoglobin.

We also examined globin gene expression in the floating cells by sequential RT-PCR (Fig. 4B). The expressions of ε-globin and ζ-globin were strongest on day 7, decreased thereafter until day 11, and were undetectable on days 13–17. In contrast, α-globin and β-major globin expression were observed from days 9 through 17. These expression patterns were similar in iPS and ES cells, suggesting that iPS cells in vitro, like ES cells, can undergo primitive followed by definitive erythropoiesis.

### Hematopoietic stem/progenitor cells develop from iPS-derived Flk-1$^+$ cells

To verify the formation of hematopoietic stem/progenitor cells in our culture system, we initially examined the expressions of c-kit, Sca1, CD34, and CD45, which are expressed by early hematopoietic progenitors (van de Rijn et al., 1989; Motro et al., 1991; Ling and Neben, 1997). FACS analysis revealed that undifferentiated iPS and ES cells expressed c-kit and Sca1, but not CD34 or CD45. Subsequent examination revealed the transient downregulation of Sca1 and c-kit on day 3, with Sca1 expression increasing again on day 5. On day 13 (8 days after cell sorting), we detected a new cell population that was positive for c-kit, Sca1, CD34, and CD45 (Fig. 5A,B).

We next investigated whether clonogenic hematopoietic cells were also produced in our culture system. Methylcellulose colony-forming assays showed that CFU-Mix, BFU-E, CFU-GM, and CFU-G colonies, as described in Materials and Methods Section, developed from the iPS-derived cells (Fig. 5C), and their numbers were not much lower than those formed by ES-derived cells (Fig. 5D). CFU-Mix and BFU-E colonies predominated the Flk-1$^+$ cells on days 7 and 9, but then

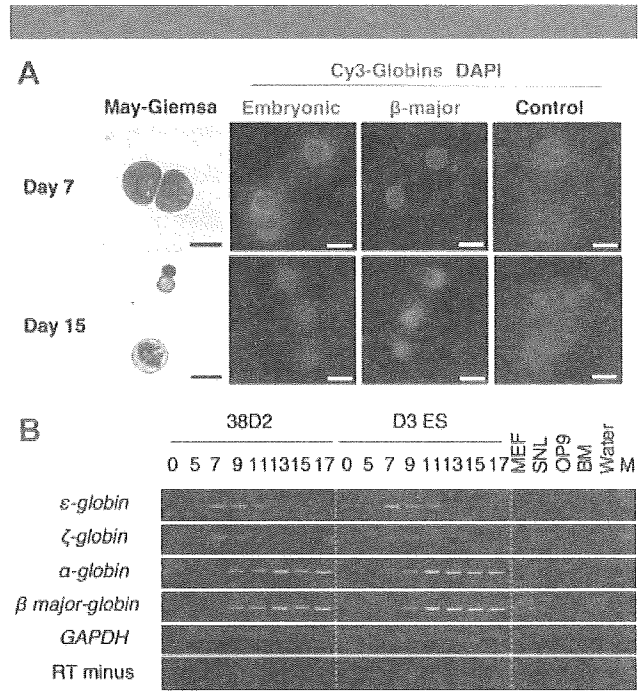


**Fig. 4. Primitive and definitive erythrocytes formed from iPS cells. A: iPS-derived floating hematopoietic cells on day 7 (upper row) and day 15 (lower row) are shown. Erythrocytes on day 7 were larger and nucleated, and strongly positive for embryonic hemoglobin, but negative for β-major globin. Red blood cells on day 15 were smaller and enucleating or enucleated, and positive for β-major globin. B: Sequential RT-PCR analysis of globin gene expressions. RNA was isolated from all cells during the initiation culture (days 0 and 5), and from floating cells during the hematopoietic culture (day 7 and thereafter). GAPDH was used as a loading control. MEF, murine embryonic fibroblasts; SNL, SNL feeder cells; OP9, OP9 feeder cells; BM, adult murine bone marrow; M, 200-bp size marker. Representative results are shown from one of three independent experiments performed on clone 38D2.**

decreased; the majority of cells after day 11 were from the CFU-GM and CFU-G colonies. These results suggest that iPS cells can generate multipotent hematopoietic progenitors almost as efficiently as ES cells.

### Concomitant development of endothelial cells from iPS-derived Flk-1$^+$ cells

We next evaluated the development of endothelial lineages in our system. At 5 days after sorting, sheet-like colonies appeared that took up Dil-acetylated low-density lipoprotein (Dil-Ac-LDL) and were positive for anti-endothelial nitric oxide synthase (eNOS), CD31, and VE-cadherin (Fig. 6A). As shown in Figure 6B, iPS-derived Flk-1$^+$ cells produced many more VE-cadherin$^+$ colonies than Flk-1$^-$ cells ($P < 0.05$).

We also analyzed the expression of the following genes that are associated with the development of hematopoietic and endothelial lineages (Fig. 6C): required for excision 1 (*Rex1*; undifferentiated cells), *Brachyury* (primitive streak and mesoderm), *Flk-1* (mesoderm), GATA-binding protein 2 (*GATA2*; hematopoietic and endothelial), *SCL* (hematopoietic), *Myb* (hematopoietic), *GATA1* (hematopoietic), and tyrosine kinase with Ig-like and endothelial growth factor-like domains 1 (*Tie1*; endothelial). Both ES and iPS cells expressed *Rex1* strongly in the undifferentiated state. *Rex1* expression gradually decreased during differentiation, and *Brachyury*, *Flk-1*, and *SCL* expressions initially appeared on day 3. Quantitative real-time PCR analyses confirmed that *Brachyury* expression increased to

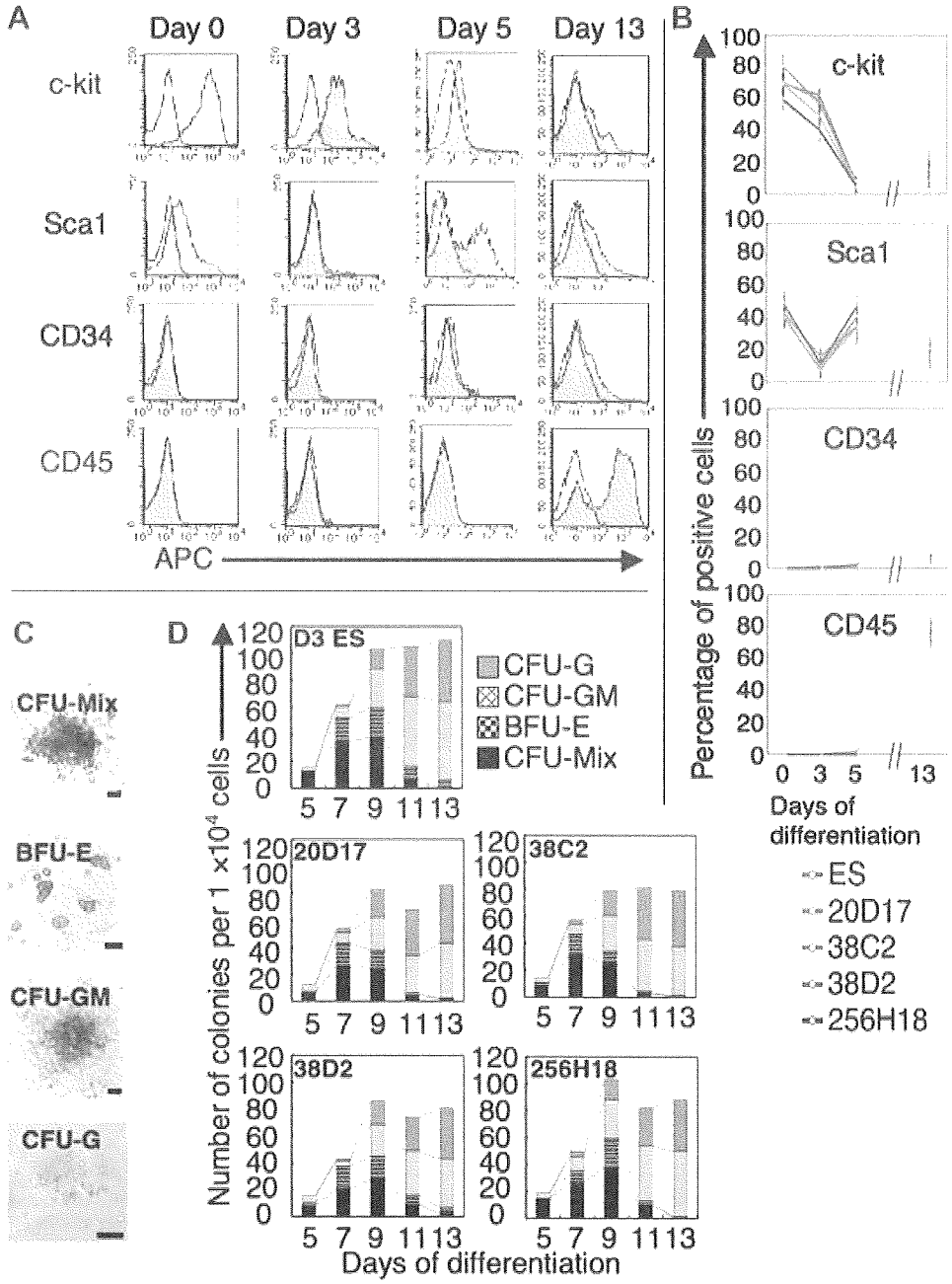


**Fig. 5. Hematopoietic stem/progenitor cells emerge from Flk-1$^+$ cells. Sequential FACS analysis of c-kit, Sca1, CD34, and CD45 in ES and iPS-derived cells during differentiation. Whole culture were harvested on indicated days and analyzed by FACS as described in Materials and Methods Section. A: Representative data from clone 38D2 are shown. Histograms show the isotype control staining profile (open bars) versus the specific antibody staining profiles (shaded bars). B: Percentages of each antigen positive cells generated from ES and iPS cells are presented as mean ± SE of three independent duplicate experiments. C: The iPS cells formed various colony types on MTC-containing medium. Data from clone 38D2 are shown as representative. Scale bars, 200 μm. D: Numbers of each colony type derived from ES and iPS cells. Data represent mean of three independent triplicate experiments.**

a maximum on day 3, followed by the upregulation of *Flk-1* and *SCL* (Fig. 6D). *Brachyury* expression continued until day 7, whereas that of *Flk-1* and *SCL* could be detected until day 9. *GATA2*, *Myb*, *GATA1*, and *Tie1* expressions were initially detected on day 5, and persisted thereafter. Taken together, these results demonstrate that, in our system, hematopoietic and/or endothelial differentiation of iPS cells occurs in a similar manner to that observed during embryogenesis.

### Common hemoangiogenic progenitors are present in iPS-derived Flk-1$^+$ populations

Previous work has demonstrated that common hemoangiogenic progenitors are present in Flk-1$^+$ cells during ES-cell differentiation (Nishikawa et al., 1998). To investigate whether iPS-derived Flk-1$^+$ cells possess the same differentiation potential, we performed a single-cell deposition

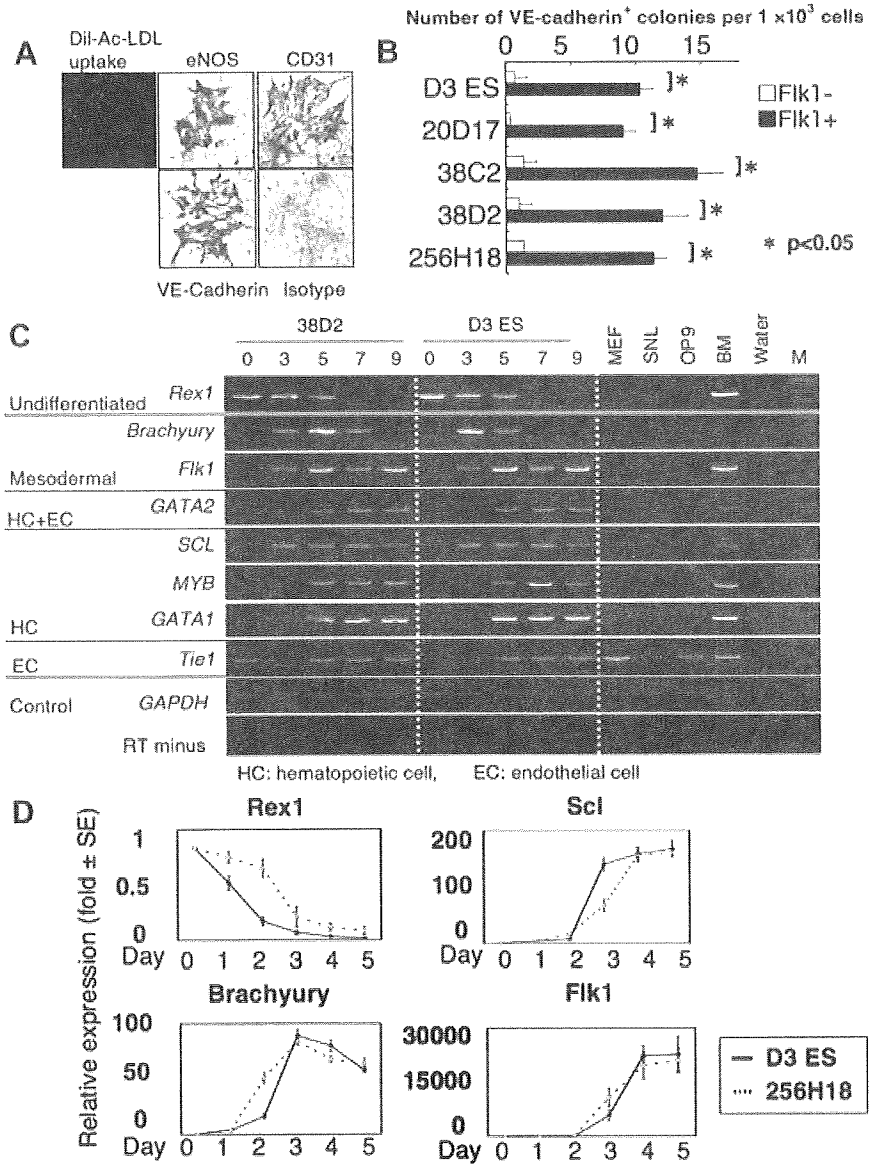


**Fig. 6. Concomitant endothelial and hematopoietic development from iPS-derived Flk-1$^+$ cells. A: The sheet-like colonies took up Dil-Ac-LDL and were positive for eNOS, CD31, and VE-cadherin. Data from clone 38D2 are shown as representative. B: Number of VE-cadherin$^+$ colonies per 1 × 10$^3$ Flk1$^+$ or Flk1$^-$ cells derived from ES and iPS cells. Data are presented as mean ± SD of three independent experiments. C: RT-PCR using mRNA isolated from ES and iPS-derived cells during culture. HC and EC means hematopoietic and endothelial cells, respectively. GAPDH was used as a loading control. M: 200 bp size marker. Representative results from one of three independent experiments performed on clone 38D2 are shown. D: The expressions of *Rex1*, *Brachyury*, *Scl*, and *Flk-1* were evaluated by real-time quantitative RT-PCR. mRNA samples were harvested from D3 ES-derived GFP$^+$ cells or clone 256H18-derived DsRed$^+$ cells sorted by FACS on indicated days. Values were normalized to *gapdh* mRNA, and the control values were arbitrarily set to day 0 (undifferentiated ES cells). Data represent the mean ± SE of three independent duplicate experiments.**

assay using the DsRed$^+$ clone 256H18. Single Flk-1$^+$ cells were deposited in four 96-well culture dishes (384 wells) containing OP9 feeder cells. Each well was observed by fluorescence microscopy 24 h after cell deposition, and wells that contained more than one DsRed$^+$ cell were excluded from further analysis. The presence of hematopoietic (Woodard et al., 2000) and endothelial (Maherali et al., 2007) colonies was confirmed not only morphologically, but also by immunostaining with a mixture of anti-CD41, CD45, and Ter119 antibodies, and anti-VE-cadherin antibodies, respectively, as previously reported (Fig. 7A) (Nishikawa et al., 1998). After 5 days of culture, the clonal outgrowth rates were 10.2% and 8.9% from 256H18 iPS and D3 ES cells, respectively. The frequencies of EC development alone, HC development alone, and HC plus EC development, respectively, were 2.7%, 5.2%, and 2.2%, respectively, from iPS cells and 2.4%, 3.5%, and 2.9%, respectively, from ES cells (Fig. 7B). Thus, the potential for mono- or bipotential progenitor development from iPS cells was almost equivalent to that from ES cells.

## Discussion

Induced PS cells may serve as a novel cell source in both research and the clinic because, like ES cells, they have an

A

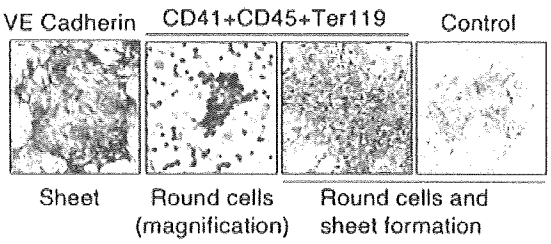


B

| Clones | Only one cell 24 hours after sorting | After 5 days | | |
|---|---|---|---|---|
| | | HC | EC | HC+EC |
| DsRed iPS cells (256H18) | 361 wells | 10 wells (2.7%) | 19 wells (5.2%) | 8 wells (2.2%) |
| D3 ES cells | 369 wells | 9 wells (2.4%) | 13 wells (3.5%) | 11 wells (2.9%) |

HC: Hematopoietic cells
EC: Endothelial cells

**Fig. 7. Common hemoangiogenic progenitors are present in Flk-1$^+$ cells during iPS-cell differentiation. A: Single Flk-1$^+$ cells were cultured on OP9 layers in the wells of 96-well plates and immunostained with anti-VE-cadherin antibodies, or a cocktail of anti-CD41, anti-CD45, and anti-Ter119 antibodies, 7 days after sorting. B: Number of wells that showed EC (endothelial cells), HC (hematopoietic cells), and EC + HC development were counted as described in text.**

unlimited capacity for self-renewal (Takahashi and Yamanaka, 2006; Meissner et al., 2007; Okita et al., 2007; Park et al., 2007; Takahashi et al., 2007; Yu et al., 2007; Aoi et al., 2008; Hanna et al., 2008; Nakagawa et al., 2008). The use of customized pluripotent stem cells would avoid the controversies surrounding ES cells. A recent study demonstrated that, after additional genetic manipulation and hematopoietic stem/progenitor cell expansion, autologous iPS cells could be used to treat mice with sickle-cell anemia, clearly revealing the advantage of these cells in regenerative medicine (Hanna et al., 2007).

One significant advantage of iPS cells is that cells from each patient can be used to screen drugs or to examine the effects of novel procedures against various diseases. Many diseases have a complex genetic etiology that affects the development, differentiation, and maturation of different tissues and organs, and require an experimental model system to faithfully reproduce their altered developmental processes (Lensch and Daley, 2006). In light of the heterogeneity of disease phenotypes and drug toxicity, it is desirable to establish defined sources of cells for drug discovery and research. In this area, immortalized cell lines and tissue-specific stem/progenitor cells that have been used for such studies are now being replaced by pluripotent stem cells.

The present study demonstrates that murine iPS cells can recapitulate early hematopoietic development in vitro. We confirmed the step-wise development of primitive and definitive hematopoietic cells, as well as endothelial cells, from Flk-1$^+$ hemoangiogenic progenitors, together with the upregulation of genes related to both lineages. Both lineages could be generated from individual Flk-1$^+$ cells, strongly suggesting the existence of common progenitor "hemangioblasts," as was previously reported for ES cells and embryos (Flamme et al., 1995; Risau, 1995; Risau and Flamme, 1995; Choi et al., 1998; Huber et al., 2004).

### Step-wise development of primitive and definitive hematopoiesis from iPS-derived intermediate mesodermal progenitors

During embryogenesis, primitive hematopoiesis emerges in the yolk sac on 7.5 d.p.c. Following this process, definitive hematopoiesis, which is the major hematopoietic process throughout life, originates on 8.5 d.p.c. in the AGM region (Muller et al., 1994; Medvinsky and Dzierzak, 1996; Matsuoka et al., 2001). When the site of hematopoiesis shifts to the fetal liver on 10.5 d.p.c. and finally to the bone marrow, the number of blood cells massively increases; erythroid cell lineages are the major products in the fetal liver, and myeloid lineages appear at later stages. Here we demonstrated that Flk-1$^+$ mesodermal cells derived from iPS cells can lead to both primitive and definitive hematopoiesis.

Interestingly, the time courses of the hematopoietic differentiation of iPS and ES cell lines in our experiments were almost precisely synchronized with those seen in embryonic development. Hematopoietic colonies on the OP9 layer were first observed on day 7 of differentiation, and the number of cells produced increased explosively from day 11. Immunostaining and RT-PCR indicated a shift from primitive to definitive hematopoiesis as differentiation progressed over time. Moreover, the results of the MTC colony-forming assay also suggested that hematopoietic differentiation in our system reflects that occurring in embryogenesis: CFU-Mix and BFU-E colonies were mainly observed until day 9, while CFU-GM and CFU-G colonies became dominant on day 11 and thereafter.

Identifying and inducing hematopoietic stem cells (HSCs) in vitro is of great biological interest. Previous studies have suggested that the cobblestone area forming cells (CAFCs) observed in the OP9 system are indicative of the existence of primitive hematopoietic progenitors (Suwabe et al., 1998); CD34, c-kit, and Sca1 are among the characteristic markers of HSCs or very immature progenitors. In our study, we observed CAFCs derived from iPS cells, and FACS analyses revealed that many of the iPS-derived hematopoietic cells expressed the progenitor markers mentioned above. Taken together, these findings suggest that iPS cells can produce very immature hematopoietic progenitors in vitro. In the future, further study will be necessary to investigate whether iPS cells can generate true HSCs that demonstrate long-term multilineage marrow reconstitution in lethally irradiated mice without any additional gene manipulation.

### Concomitant differentiation of iPS cells into hematopoietic and endothelial lineages

Several in vivo and in vitro studies have demonstrated a close association between hematopoietic and endothelial differentiation. Previous experiments have shown that murine and primate ES cells differentiate into hematopoietic cells via common Flk1$^+$ hemoangiogenic progenitors (Nishikawa et al., 1998; Umeda et al., 2006). Using RT-PCR and the single-cell deposition assay, our study demonstrated that iPS cells, like ES cells, can generate hematopietic and endothelial cells concomitantly, as is observed in embryogenesis.

The RT-PCR data demonstrated that the expression of the early mesodermal marker *Brachyury* was followed by that of *flk-1* and *scl*, both of which are crucial for the development of common progenitors (Nishikawa et al., 1998; Chung et al., 2002). The expression of genes associated with both lineages began thereafter. These results suggest that the orchestrated process from mesoderm development to the specification of either lineage during embryogenesis is also recapitulated in the iPS-cell model.

The single-deposition assay demonstrated that iPS cells possess an equivalent capacity to ES cells to develop bipotent progenitors at the single cell level. However, the frequency of progenitor development was unexpectedly low. One possible reason for this is the low clonal growth rate in our single-cell culture condition. Another possibility is that the sorted Flk-1$^+$ cells included, besides hemangioblasts, progenitors that contribute to other mesodermal lineages. Recent studies on murine ES and iPS cells demonstrated the development of cardiac muscles, vascular smooth muscles, and pericytes from Flk-1$^+$ fractions (Yamashita et al., 2000; Iida et al., 2005; Baba et al., 2007b; Narazaki et al., 2008). We also observed the formation of contractile colonies from Flk-1$^+$ fractions (data not shown). This may be one alternative reason for the observed low frequency of differentiation of either lineage. Further studies will enhance our understanding of the developmental biology of iPS cells.

### Hematopoietic potential of iPS-derived Flk-1$^+$ progenitors is equivalent, regardless of the clone

In our experiments, the efficacy of Flk-1$^+$ cell induction varied between the clones, although the timing of their differentiation was the same. This may be potentially due to contamination by the SNL feeder cells. As these feeder cells were not eliminated at the start of differentiation, they would have remained throughout the assay and might have inhibited differentiation. However, to address these problems, it will be necessary to study the biological characteristics of iPS cells further, including their epigenetic behavior during differentiation. The most interesting and encouraging finding in our study was that the sorted Flk-1$^+$ cells derived from all analyzed iPS and ES clones were similar in their ability to generate hematopoietic cells.

In conclusion, our results demonstrate that iPS cells can develop into hematopoietic cells in vitro via hemoangiogenic progenitors, the so-called "hemangioblasts." Furthermore, iPS cells traverse the primitive and definitive hematopoietic stages in a manner similar to that observed during embryogenesis. Although future investigations at the biological and molecular levels are highly desirable, our study suggests that iPS cells hold great promise in medicine, and may aid in attaining the long sought goal of patient-specific stem cells.

## Acknowledgments

This work was supported by grants from the Ministry of Education, Culture, Sports, Science, and Technology of Japan.

## Literature Cited

Aoi T, Yae K, Nakagawa M, Ichisaka T, Okita K, Takahashi K, Chiba T, Yamanaka S. 2008. Generation of pluripotent stem cells from adult mouse liver and stomach cells. Science (New York, NY) 321:699–702.

Baba S, Heike T, Umeda K, Iwasa T, Kaichi S, Hiraumi Y, Doi H, Yoshimoto M, Kanatsu-Shinohara M, Shinohara T, Nakahata T. 2007a. Generation of cardiac and endothelial cells from neonatal mouse testis-derived multipotent germline stem cells. Stem Cells (Dayton, Ohio) 25:1375–1383.

Baba S, Heike T, Yoshimoto M, Umeda K, Doi H, Iwasa T, Lin X, Matsuoka S, Komeda M, Nakahata T. 2007b. Flk1(+) cardiac stem/progenitor cells derived from embryonic stem cells improve cardiac function in a dilated cardiomyopathy mouse model. Cardiovasc Res 76:119–131.

Choi K, Kennedy M, Kazarov A, Papadimitriou JC, Keller G. 1998. A common precursor for hematopoietic and endothelial cells. Development (Cambridge, England) 125:725–732.

Chung YS, Zhang WJ, Arentson E, Kingsley PD, Palis J, Choi K. 2002. Lineage analysis of the hemangioblast as defined by FLK1 and SCL expression. Development (Cambridge, England) 129:5511–5520.

Doetschman TC, Eistetter H, Katz M, Schmidt W, Kemler R. 1985. The in vitro development of blastocyst-derived embryonic stem cell lines: Formation of visceral yolk sac, blood islands and myocardium. J Embryol Exp Morphol 87:27–45.

Evans MJ, Kaufman MH. 1981. Establishment in culture of pluripotential cells from mouse embryos. Nature 292:154–156.

Flamme I, Breier G, Risau W. 1995. Vascular endothelial growth factor (VEGF) and VEGF receptor 2 (flk-1) are expressed during vasculogenesis and vascular differentiation in the quail embryo. Dev Biol 169:699–712.

Garcia-Porrero JA, Manaia A, Jimeno J, Lasky LL, Dieterlen-Lievre F, Godin IE. 1998. Antigenic profiles of endothelial and hemopoietic lineages in murine intraembryonic hemogenic sites. Dev Comp Immunol 22:303–319.

Hanna J, Wernig M, Markoulaki S, Sun CW, Meissner A, Cassady JP, Beard C, Brambrink T, Wu LC, Townes TM, Jaenisch R. 2007. Treatment of sickle cell anemia mouse model with iPS cells generated from autologous skin. Science (New York, NY) 318:1920–1923.

Hanna J, Markoulaki S, Schorderet P, Carey BW, Beard C, Wernig M, Creyghton MP, Steine EJ, Cassady JP, Foreman R, Lengner CJ, Dausman JA, Jaenisch R. 2008. Direct reprogramming of terminally differentiated mature B lymphocytes to pluripotency. Cell 133:250–264.

Hansen JN, Konkel DA, Leder P. 1982. The sequence of a mouse embryonic beta-globin gene. Evolution of the gene and its signal region. J Biol Chem 257:1048–1052.

Huber TL, Kouskoff V, Fehling HJ, Palis J, Keller G. 2004. Haemangioblast commitment is initiated in the primitive streak of the mouse embryo. Nature 432:625–630.

Iida M, Heike T, Yoshimoto M, Baba S, Doi H, Nakahata T. 2005. Identification of cardiac stem cells with FLK1, CD31, and VE-cadherin expression during embryonic stem cell differentiation. FASEB J 19:371–378.

Jackson CW. 1973. Cholinesterase as a possible marker for early cells of the megakaryocytic series. Blood 42:413–421.

Jaenisch R, Young R. 2008. Stem cells, the molecular circuitry of pluripotency and nuclear reprogramming. Cell 132:567–582.

Konkel DA, Tilghman SM, Leder P. 1978. The sequence of the chromosomal mouse beta-globin major gene: Homologies in capping, splicing and poly(A) sites. Cell 15:1125–1132.

Ku HT, Zhang N, Kubo A, O'Connor R, Mao M, Keller G, Bromberg JS. 2004. Committing embryonic stem cells to early endocrine pancreas in vitro. Stem Cells (Dayton, Ohio) 22:1205–1217.

Kyba M, Perlingeiro RC, Daley GQ. 2002. HoxB4 confers definitive lymphoid-myeloid engraftment potential on embryonic stem cell and yolk sac hematopoietic progenitors. Cell 109:29–37.

Kyba M, Perlingeiro RC, Hoover RR, Lu CW, Pierce J, Daley GQ. 2003. Enhanced hematopoietic differentiation of embryonic stem cells conditionally expressing Stat5. Proc Natl Acad Sci USA 100:11904–11910.

Leder A, Weir L, Leder P. 1985. Characterization, expression, and evolution of the mouse embryonic zeta-globin gene. Mol Cell Biol 5:1025–1033.

Leder A, Kuo A, Shen MM, Leder P. 1992. In situ hybridization reveals co-expression of embryonic and adult alpha globin genes in the earliest murine erythrocyte progenitors. Development (Cambridge, England) 116:1041–1049.

Lensch MW, Daley GQ. 2006. Scientific and clinical opportunities for modeling blood disorders with embryonic stem cells. Blood 107:2605–2612.

Ling V, Neben S. 1997. In vitro differentiation of embryonic stem cells: Immunophenotypic analysis of cultured embryoid bodies. J Cell Physiol 171:104–115.

Maherali N, Sridharan R, Xie W, Utikal J, Eminli S, Arnold K, Stadtfeld M, Yachechko R, Tchieu J, Jaenisch R, Plath K, Hochedlinger K. 2007. Directly reprogrammed fibroblasts show global epigenetic remodeling and widespread tissue contribution. Cell Stem Cell 1:55–70.

Matsuoka S, Tsuji K, Hisakawa H, Xu M, Ebihara Y, Ishii T, Sugiyama D, Manabe A, Tanaka R, Ikeda Y, Asano S, Nakahata T. 2001. Generation of definitive hematopoietic stem cells from murine early yolk sac and paraaortic splanchnopleures by aorta-gonad-mesonephros region-derived stromal cells. Blood 98:6–12.

Medvinsky A, Dzierzak E. 1996. Definitive hematopoiesis is autonomously initiated by the AGM region. Cell 86:897–906.

Meissner A, Wernig M, Jaenisch R. 2007. Direct reprogramming of genetically unmodified fibroblasts into pluripotent stem cells. Nat Biotechnol 25:1177–1181.

Miwa Y, Atsumi T, Imai N, Ikawa Y. 1991. Primitive erythropoiesis of mouse teratocarcinoma stem cells PCC3/A/1 in serum-free medium. Development (Cambridge, England) 111:543–549.

Moore MA, Metcalf D. 1970. Ontogeny of the haemopoietic system: Yolk sac origin of in vivo and in vitro colony forming cells in the developing mouse embryo. Br J Haematol 18:279–296.

Motro B, van der Kooy D, Rossant J, Reith A, Bernstein A. 1991. Contiguous patterns of c-kit and steel expression: Analysis of mutations at the W and Sl loci. Development (Cambridge, England) 113:1207–1221.

Muller AM, Medvinsky A, Strouboulis J, Grosveld F, Dzierzak E. 1994. Development of hematopoietic stem cell activity in the mouse embryo. Immunity 1:291–301.

Nakagawa M, Koyanagi M, Tanabe K, Takahashi K, Ichisaka T, Aoi T, Okita K, Mochiduki Y, Takizawa N, Yamanaka S. 2008. Generation of induced pluripotent stem cells without Myc from mouse and human fibroblasts. Nat Biotechnol 26:101–106.

Nakahata T, Ogawa M. 1982a. Clonal origin of murine hemopoietic colonies with apparent restriction to granuclocyte-macrophage-megakaryocyte (GMM) differentiation. J Cell Physiol 111:239–246.

Nakahata T, Ogawa M. 1982b. Hemopoietic colony-forming cells in umbilical cord blood with extensive capability to generate mono- and multipotential hemopoietic progenitors. J Clin Invest 70:1324–1328.

Nakahata T, Ogawa M. 1982c. Identification in culture of a class of hemopoietic colony-forming units with extensive capability to self-renew and generate multipotential hemopoietic colonies. Proc Natl Acad Sci USA 79:3843–3847.

Nakanishi M, Kurisaki A, Hayashi Y, Warashina M, Ishiura S, Kusuda-Furue M, Asashima M. 2009. Directed induction of anterior and posterior primitive streak by Wnt from embryonic stem cells cultured in a chemically defined serum-free medium. FASEB J 23:114–122.

Nakano T, Kodama H, Honjo T. 1994. Generation of lymphohematopoietic cells from embryonic stem cells in culture. Science (New York, NY) 265:1098–1101.

Nakano T, Kodama H, Honjo T. 1996. In vitro development of primitive and definitive erythrocytes from different precursors. Science (New York, NY) 272:722–724.

Narazaki G, Uosaki H, Teranishi M, Okita K, Kim B, Matsuoka S, Yamanaka S, Yamashita JK. 2008. Directed and systematic differentiation of cardiovascular cells from mouse induced pluripotent stem cells. Circulation 118:498–506.

Nishikawa SI, Nishikawa S, Hirashima M, Matsuyoshi N, Kodama H. 1998. Progressive lineage analysis by cell sorting and culture identifies FLK1+VE-cadherin+ cells at a diverging point of endothelial and hemopoietic lineages. Development (Cambridge, England) 125:1747–1757.

Nishioka Y, Leder P. 1979. The complete sequence of a chromosomal mouse alpha-globin gene reveals elements conserved throughout vertebrate evolution. Cell 18:875–882.

Okita K, Ichisaka T, Yamanaka S. 2007. Generation of germline-competent induced pluripotent stem cells. Nature 448:313–317.

Park IH, Zhao R, West JA, Yabuuchi A, Huo H, Ince TA, Lerou PH, Lensch MW, Daley GQ. 2007. Reprogramming of human somatic cells to pluripotency with defined factors. Nature 451:141–146.

Redmond LC, Dumur CI, Archer KJ, Haar JL, Lloyd JA. 2008. Identification of erythroid-enriched gene expression in the mouse embryonic yolk sac using microdissected cells. Dev Dyn 237:436–446.

Risau W. 1995. Differentiation of endothelium. FASEB J 9:926–933.
Risau W, Flamme I. 1995. Vasculogenesis. Annu Rev Cell Dev Biol 11:73–91.
Shalaby F, Ho J, Stanford WL, Fischer KD, Schuh AC, Schwartz L, Bernstein A, Rossant J. 1997. A requirement for Flk1 in primitive and definitive hematopoiesis and vasculogenesis. Cell 89:981–990.
Shimizu R, Takahashi S, Ohneda K, Engel JD, Yamamoto M. 2001. In vivo requirements for GATA-1 functional domains during primitive and definitive erythropoiesis. EMBO J 20:5250–5260.
Shimizu R, Kuroha T, Ohneda O, Pan X, Ohneda K, Takahashi S, Philipsen S, Yamamoto M. 2004. Leukemogenesis caused by incapacitated GATA-1 function. Mol Cell Biol 24:10814–10825.
Shinoda G, Umeda K, Heike T, Arai M, Niwa A, Ma F, Suemori H, Luo HY, Chui DH, Torii R, Shibuya M, Nakatsuji N, Nakahata T. 2007. alpha4-Integrin(+) endothelium derived from primate embryonic stem cells generates primitive and definitive hematopoietic cells. Blood 109:2406–2415.
Suwabe N, Takahashi S, Nakano T, Yamamoto M. 1998. GATA-1 regulates growth and differentiation of definitive erythroid lineage cells during in vitro ES cell differentiation. Blood 92:4108–4118.
Takahashi K, Yamanaka S. 2006. Induction of pluripotent stem cells from mouse embryonic and adult fibroblast cultures by defined factors. Cell 126:663–676.
Takahashi K, Tanabe K, Ohnuki M, Narita M, Ichisaka T, Tomoda K, Yamanaka S. 2007. Induction of pluripotent stem cells from adult human fibroblasts by defined factors. Cell 131:861–872.
Umeda K, Heike T, Yoshimoto M, Shiota M, Suemori H, Luo HY, Chui DH, Torii R, Shibuya M, Nakatsuji N, Nakahata T. 2004. Development of primitive and definitive hematopoiesis from nonhuman primate embryonic stem cells in vitro. Development (Cambridge, England) 131:1869–1879.
Umeda K, Heike T, Yoshimoto M, Shinoda G, Shiota M, Suemori H, Luo HY, Chui DH, Torii R, Shibuya M, Nakatsuji N, Nakahata T. 2006. Identification and characterization of hemoangiogenic progenitors during cynomolgus monkey embryonic stem cell differentiation. Stem Cells (Dayton, Ohio) 24:1348–1358.
van de Rijn M, Heimfeld S, Spangrude GJ, Weissman IL. 1989. Mouse hematopoietic stem-cell antigen Sca-1 is a member of the Ly-6 antigen family. Proc Natl Acad Sci USA 86:4634–4638.
Vodyanik MA, Slukvin II. 2007. Hematoendothelial differentiation of human embryonic stem cells. Curr Protoc Cell Biol Chapter 23:Unit 23.6.
Vodyanik MA, Bork JA, Thomson JA, Slukvin II. 2005. Human embryonic stem cell-derived CD34+ cells: Efficient production in the coculture with OP9 stromal cells and analysis of lymphohematopoietic potential. Blood 105:617–626.
Wood HB, May G, Healy L, Enver T, Morriss-Kay GM. 1997. CD34 expression patterns during early mouse development are related to modes of blood vessel formation and reveal additional sites of hematopoiesis. Blood 90:2300–2311.
Woodard JP, Gulbahce E, Shreve M, Steiner M, Peters C, Hite S, Ramsay NK, DeFor T, Baker KS. 2000. Pulmonary cytolytic thrombi: A newly recognized complication of stem cell transplantation. Bone Marrow Transplant 25:293–300.
Xu MJ, Matsuoka S, Yang FC, Ebihara Y, Manabe A, Tanaka R, Eguchi M, Asano S, Nakahata T, Tsuji K. 2001. Evidence for the presence of murine primitive megakaryocytopoiesis in the early yolk sac. Blood 97:2016–2022.
Yamashita J, Itoh H, Hirashima M, Ogawa M, Nishikawa S, Yurugi T, Naito M, Nakao K. 2000. Flk1-positive cells derived from embryonic stem cells serve as vascular progenitors. Nature 408:92–96.
Yang FC, Tsuji K, Oda A, Ebihara Y, Xu MJ, Kaneko A, Hanada S, Mitsui T, Kikuchi A, Manabe A, Watanabe S, Ikeda Y, Nakahata T. 1999. Differential effects of human granulocyte colony-stimulating factor (hG-CSF) and thrombopoietin on megakaryopoiesis and platelet function in hG-CSF receptor-transgenic mice. Blood 94:950–958.
Yu J, Vodyanik MA, Smuga-Otto K, Antosiewicz-Bourget J, Frane JL, Tian S, Nie J, Jonsdottir GA, Ruotti V, Stewart R, Slukvin II, Thomson JA. 2007. Induced pluripotent stem cell lines derived from human somatic cells. Science (New York, NY) 318:1917–1920.

Clinical & Experimental Immunology
The Journal of Translational Immunology

Clinical and Experimental Immunology ORIGINAL ARTICLE doi:10.1111/j.1365-2249.2009.04073.x

# Unique activation status of peripheral blood mononuclear cells at acute phase of Kawasaki disease

K. Ikeda,* K. Yamaguchi,* T. Tanaka,* Y. Mizuno,† A. Hijikata,‡ O. Ohara,‡ H. Takada,* K. Kusuhara§ and T. Hara*

*Department of Pediatrics, Graduate School of Medical Sciences, Kyushu University, †Fukuoka Children's Hospital and Medical Center for Infectious Disease, Fukuoka, ‡Laboratory for Immunogenomics, RIKEN Research Center for Allergy and Immunology, Yokohama, and §Department of Pediatrics, University of Occupational and Environmental Medicine, Kitakyushu, Japan

Accepted for publication 9 November 2009
Correspondence: K. Ikeda, Department of Pediatrics, Graduate School of Medical Sciences, Kyushu University, 3-1-1 Maidashi, Higashi-ku, Fukuoka 812-8582, Japan.
E-mail: ikeq@pediatr.med.kyushu-u.ac.jp

## Summary

Although Kawasaki disease (KD) is characterized by a marked activation of the immune system with elevations of serum proinflammatory cytokines and chemokines at acute phase, the major sources for these chemical mediators remain controversial. We analysed the activation status of peripheral blood mononuclear cells (PBMCs) by flow cytometry, DNA microarray and quantitative reverse transcription–polymerase chain reaction. The proportions of $CD69^+$ cells in both natural killer cells and γδT cells at acute-phase KD were significantly higher than those at convalescent-phase KD. Microarray analysis revealed that five genes such as *NAIP*, *IPAF*, *S100A9*, *FCGR1A* and *GCA* up-regulated in acute-phase KD and the pathways involved in acute phase KD were related closely to the innate immune system. The relative expression levels of damage-associated molecular pattern molecule (DAMP) (*S100A9* and *S100A12*) genes in PBMCs at acute-phase KD were significantly higher than those at convalescent-phase KD, while those of *TNFA*, *IL1B* and *IL6* genes were not significantly different between KD patients and healthy controls. Intracellular production of tumour necrosis factor-α, interlaukin-10 and interferon-γ in PBMCs was not observed in KD patients. The present data have indicated that PBMCs showed a unique activation status with high expression of DAMP genes but low expression of proinflammatory cytokine genes, and that the innate immune system appears to play a role in the pathogenesis and pathophysiology of KD.

**Keywords:** acquired immunity, cytokines, innate immunity, Kawasaki disease, peripheral blood mononuclear cells

## Introduction

Kawasaki disease (KD) is an acute febrile illness of childhood with systemic vasculitis characterized by the occurrence of coronary arteritis. Although KD is characterized by a marked activation of the immune system with elevations of serum proinflammatory cytokines and chemokines at acute phase [1–3], no previous studies have demonstrated that peripheral blood mononuclear cells (PBMCs) serve as the major sources for these chemical mediators. Although the activation of monocytes/macrophages has been reported to have an important role at acute phase of KD [4], there were no significant differences in the expression levels of *IL6*, *IL8* and *TNFA* genes in separated monocytes before and after high-dose gammaglobulin therapy [5].

Activation status of PBMCs, especially T cells, at acute phase of KD is also controversial. In a previous report, it has been thought that most activated T cells moved to local tissues from peripheral blood at acute phase and returned from there at convalescent phase [3]. Although numerous immunological studies on T cells have been reported, no previous studies analysed T cells by separating them into two distinct populations, αβT cells and γδT cells, which are involved mainly in acquired and innate immunity, respectively.

To clarify the pathophysiology of KD, we analysed the activation status of PBMCs including αβT cells, γδT cells, natural killer (NK) cells and B cells by flow cytometry, DNA microarray and quantitative reverse transcription–polymerase chain reaction (RT–PCR). These analyses have shown consistently that the innate immune system might be involved in the pathogenesis and pathophysiology of KD, and that PBMCs were not a major source for proinflammatory cytokines such as interleukin (IL)-6 and tumour necrosis factor (TNF) in acute-phase KD sera.

 

## Materials and methods

### Patients

All patients enrolled in this study were admitted to the Kyushu University Hospital or Fukuoka Children's Hospital between April 2005 and February 2009. The patient group consisted of 51 KD patients who met the criteria for the Diagnostic Guidelines of Kawasaki Disease (http://www.kawasaki-disease.org/diagnostic/index.html). A coronary artery was defined as abnormal if the luminal diameter was greater than 3 mm in children aged less than 5 years (greater than 4 mm in children older than 5 years), if the internal diameter of a segment was at least 1·5 times as large as that of an adjacent segment, or if the lumen was irregular [6]. All patients received oral aspirin (30 mg/kg/day) and 1–2 g/kg of intravenous immunoglobulin (IVIG) as an initial treatment.

To analyse immunological profiles in KD by flow cytometry, we recruited 38 KD patients (median age, 2·0 years; range, 3 months–7·3 years) between September 2006 and August 2008. No patients had coronary artery lesions (CAL). We first analysed the proportions of activated T, B and NK cells in the peripheral blood of both seven patients with KD and 15 age-matched healthy controls by flow cytometry. CD69, human leucocyte antigen D-related (HLA-DR) and CD25 were used as activation markers. These cells were analysed before treatment with IVIG (median day of illness, day 5; range, days 3–6) and in the convalescent phase (median day of illness, day 13; range, days 13–18). To analyse further the immunological profiles in KD, the proportion of $CD69^+$ cells were investigated in αβT cells ($n = 23$), γδT cells ($n = 23$), NK cells ($n = 35$) and B cells ($n = 35$).

To analyse mRNA expression levels, blood samples were obtained prior to the treatment (on 4–5 days of illness) from three KD patients (median age, 4·7 years; range, 4·1–5·3 years) without CAL and from five healthy adults. PBMCs were separated from peripheral blood and were used for cDNA microarray analysis.

To analyse mRNA expression levels using quantitative real-time RT–PCR, blood samples were obtained from 10 to 16 KD patients (median age, 1·7 years; range; 4 months–7·2 years) in both acute and convalescent phase, and from 20 age-matched control subjects including nine patients (median age, 2·6 years; range, 5 months–13·1 years) with active infections [three patients with bacterial meningitis (one *Haemophilus influenzae* type b, one *Streptococcus pneumoniae* and one unknown), six patients with viral infection (three measles, three Epstein–Barr virus infection)] and 11 healthy children (median age, 5·0 years; range, 1·7–7·6 years).

All subjects gave written informed consent for this study, according to the process approved by the Ethical Committee of Kyushu University and Fukuoka Children's Hospital and Medical Center for Infectious Diseases, Fukuoka, Japan.

### Total RNA extraction and RNA amplification

PBMCs were separated from peripheral blood by density-gradient centrifugation using lymphocyte separation medium (Cappel-ICN Immunobiologicals, Costa Mesa, CA, USA) containing 6·2 g Ficoll and 9·4 g sodium diatrizoate per 100 ml. Total RNA was extracted from these cells using an RNA extraction kit (Isogen; Nippon Gene, Osaka, Japan), according to the manufacturer's instructions. Total RNAs from five healthy adults were mixed. An amino allyl message amp aRNA Kit (Ambion, Austin, TX, USA) was used to amplify the total RNA. Briefly, double-stranded complementary DNA (cDNA) was synthesized from total RNA using oligo-dT primer with a T7 RNA polymerase promoter site added to the 3′ end. Then, *in vitro* transcription was performed in the presence of amino allyl uridine-5′-triphosphate (UTP) to produce multiple copies of amino allyl-labelled complementary RNA (cRNA). Amino allyl-labelled cRNA was purified, and then reacted with N-hydroxy succinimide esters of Cy3 (Amersham Pharmacia Biotech, Piscataway, NJ, USA) for cRNA from PBMCs of healthy controls, and Cy5 (Amersham Pharmacia Biotech) for that from PBMCs of the acute-phase KD patients, according to the protocol of Hitachi Software Engineering (Yokohama, Japan).

### Microarray analysis

Microarray analysis for PBMCs of acute-phase KD patients was performed using an AceGene Human Oligo Chip 30K (Hitachi Software Engineering) that contains approximately 30 000 genes. The arrays were scanned by FLA-8000 (Fuji Photo Film, Tokyo, Japan), and changed to the numerical values by ArrayVision (Amersham Biosciences). The numerical data were normalized using the LOWESS method. In the microarray analysis of PBMCs, data from three KD patients and those from five healthy controls were compared. Genes that were up-regulated consistently in KD patients compared with healthy controls, and that showed more than a threefold difference by the comparison between the two groups in the mean expression levels, were selected. The data with low signal-to-noise ratios (S/N < 3) were not used for further analysis. The data were analysed using Gene Spring software (Silicon Genetics, Redwood City, CA, USA).

### Accession number

GSE17975 (Gene Expression Omnibus).

### Pathway analysis of microarray results

To understand the underlying phenomenon in the acute phase of KD, a system biology approach was performed using microarray data. Genes were selected as follows: (i)

data with low signal-to-noise ratios (S/N < 3) were excluded; (ii) the mean expression ratio between three KD patients and five healthy controls was more than 1·0 $\log_2$, or less than −1·0 $\log_2$; and (iii) if two or more probes represented the same gene, probes with maximum mean fold-change values were selected. Selected genes were put into Pathway-Express in Onto-Tools (http://vortex.cs.wayne.edu). Pathway-Express searches the Kyoto Encyclopedia of Genes and Genomes (KEGG) pathway database (http://www.genome.ad.jp/) for each input gene, and the impact analysis was performed in order to build a list of all associated pathways [7–9]. An impact factor (IF) is calculated for each pathway incorporating parameters, such as the normalized fold change of the differentially expressed genes, the statistical significance of the set of pathway genes and the topology of the signalling pathway [8]. The corrected gamma *P*-value is the *P*-value provided by the impact analysis. The differences were considered to be significant when the corrected gamma *P*-value was less than 0·05.

### Quantitative real-time RT–PCR

Total RNA was extracted from cell pellets of PBMCs using the same method as used in the microarray analysis, followed by cDNA synthesis using a first-strand cDNA synthesis kit (GE Healthcare UK Ltd, Buckinghamshire, UK) with random hexamers. *S100A9*, *S100A12*, *TNFA*, *IL1B*, *IL8* and *IL6* mRNA expression levels were analysed by *Taq*Man® gene expression assays Hs00610058_m1, Hs00194525_m1, Hs00174128_m1, Hs99999029_m1, Hs99999034_m1 and Hs99999032_m1 (Applied Biosystems, Foster City, CA, USA). These products consisted of a 20× mix of unlabelled PCR primers and a *Taq*Man MGB probe (FAMTM dye-labelled). A *Taq*Man human glyceraldehyde-3-phosphate-dehydrogenase (GAPDH) control reagent kit (Applied Biosystems) was used as an internal control. These *Taq*Man probes were labelled with the quencher fluor-6-carboxy-tetramethyl rhodamine (emission I, 582 nm) at the 3′ end through a linker-arm nucleotide. The mRNA expression levels of the targeted and GAPDH genes were quantified by an ABI PRISM 7700 sequence detector (Applied Biosystems), as described previously [10]. A comparative threshold cycle (CT) was used to determine gene expression levels relative to those of the no-tissue control (calibrator). Hence, steady-state mRNA levels were expressed as an *n*-fold difference relative to the calibrator, as described previously [11]. To calculate the relative expression level in cells, the level of gene expression was divided by that of the GAPDH. All experiments were carried out in duplicate and repeated for confirmation.

### Flow cytometry

Ethylenediamine tetraacetic acid (EDTA) blood samples were collected from both patients and controls. The proportions of $CD69^+$ cells were analysed within 12 h after sampling by using an EPICS XL (Beckman Coulter, Fullteron, CA, USA), as described previously [10]. The proportions of HLA-$DR^+$ or $CD25^+$ cells were also analysed within 24 h. The forward and side light-scatter gate was set to analyse viable cells and to exclude background artefacts. Multi-colour staining was carried out with fluorescein isothiocyanate (FITC)-, phycoerythrin (PE)- or PE-cyanin 5·1 (PC5)-conjugated monoclonal antibodies against CD3, CD16, CD19, CD25, CD56, CD69, HLA-DR and T cell receptor (TCR)γδ (Beckman Coulter). Three-colour flow cytometric analysis was performed on cells within the lymphocyte light-scatter gate using forward and side scatters. Heparinized whole blood samples from five healthy controls were preincubated with or without lipopolysaccharide (LPS) or phorbol 12-myristate 13-acetate (PMA) and ionomycin for 4 h at 37°C under a 95% humidified air with 5% $CO_2$, and intracellular tumour necrosis factor (TNF)-α, IL-10 or interferon (IFN)-γ staining was performed using the Fastimmune Intracellular Staining System (BD Bioscience Pharmingen, San Diego, CA, USA) [12]. The analysis gate was set for monocytes or T cells by side scatter, and CD14 or CD3 expression. Intracellular TNF-α, IL-10 and IFN-γ staining in peripheral blood cells from seven KD patients was performed using the same system, without *in vitro* stimulation.

## Results

### Flow cytometric analysis of the activation markers on T, B and NK cells at acute phase of KD

We first analysed the proportions of activated T, B and NK cells in the peripheral blood of KD patients by flow cytometry. CD69, HLA-DR and CD25 were used as activation markers. As shown in Fig. 1a, the proportions of $CD69^+$ T cells were significantly higher at acute phase than those at convalescent phase of KD, while those of $CD69^+$ B cells were more prominent at convalescent phase than at acute phase of KD ($P < 0{\cdot}01$). The proportions of $CD69^+$ cells in $CD56^+CD16^+$ and $CD16^+CD56^-$ NK cells at acute phase of KD were significantly higher than those at convalescent phase of KD. The proportions of $CD69^+$ cells in $CD56^+CD16^-$ NK cells and the proportions of $CD25^+$ or HLA-$DR^+$ cells in T cells, B cells or all three NK cell subsets were not significantly different between the two phases of KD.

To analyse further T cell activation in KD, the proportion of $CD69^+$ cells were investigated through the separation of T cells to αβ and γδT cells, which are involved in acquired and innate immunity, respectively. As shown in Fig. 1b and c, the proportions of $CD69^+$ cells in γδT cells at acute phase of KD were significantly higher than those at convalescent phase of KD (median values: 17·9% at acute phase *versus* 7·9% at convalescent phase in γδ T cells, $P < 0{\cdot}0005$). Conversely, the activation of αβ T cells was minimal in terms of CD69

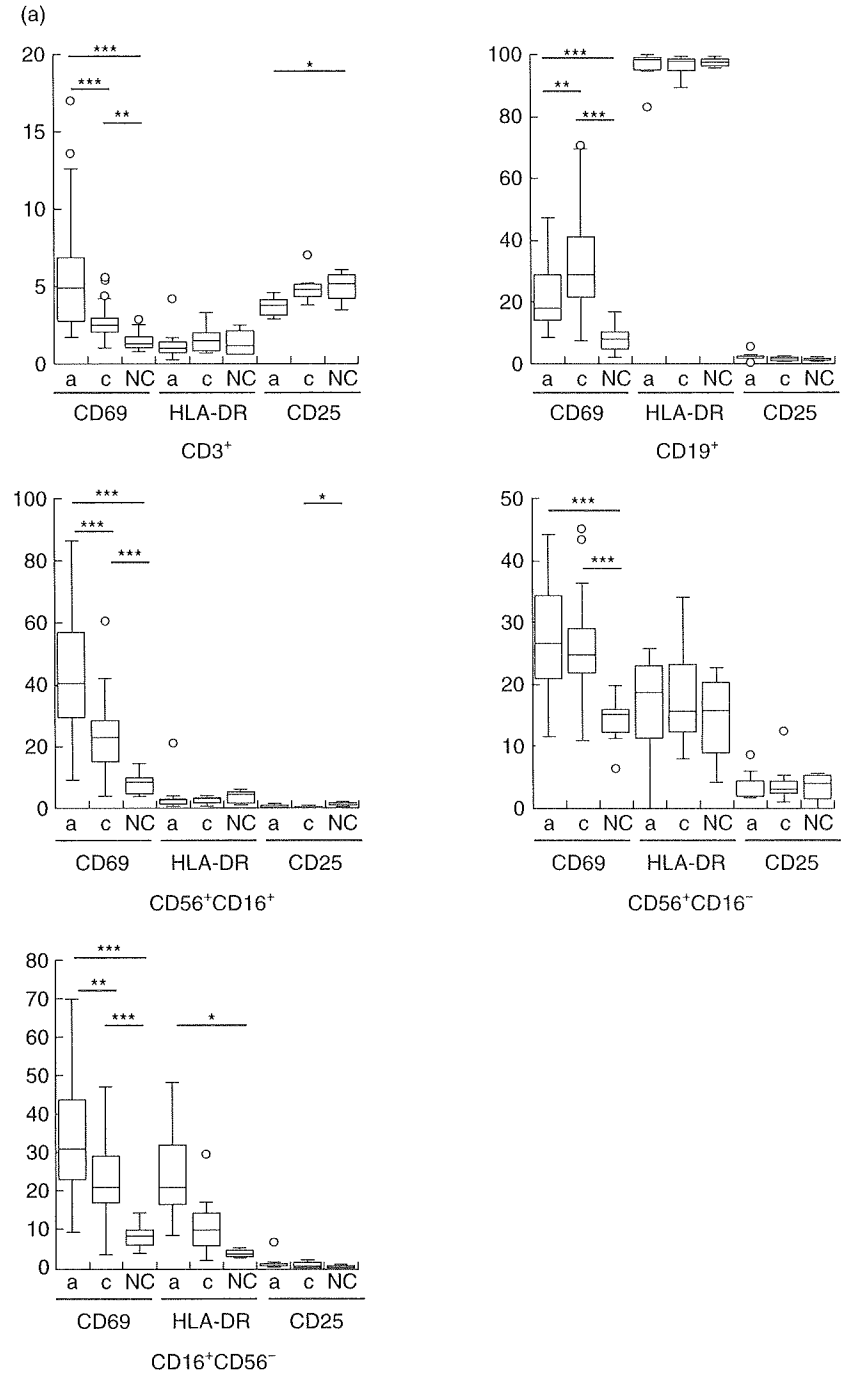


**Fig. 1.** Flow cytometric analysis of the activation markers on T, B and natural killer (NK) cells at acute phase of Kawasaki disease (KD). (a) The proportions of activated T, B and NK cells in the peripheral blood of seven patients with KD and 15 healthy control subjects were analysed by flow cytometry. CD69, human leucocyte antigen D-related (HLA-DR) and CD25 were used as activation markers. $^{*}P \leq 0{\cdot}05$; $^{**}P \leq 0{\cdot}01$; $^{***}P \leq 0{\cdot}0001$. (a) Acute phase; (c) convalescent phase; NC, healthy controls. The form of box-plot is as follows. The bottom and the top of the box correspond to 25th and 75th percentile points, respectively. The line within the box represents the median, and the whiskers indicate the values of 10th and 90th percentiles. (b,c) Representative density plot of flow cytometric analysis of $CD69^{+}$ cells on NK, T and B cells (b) and the proportions of $CD69^{+}$ cells in αβ and γδ T cells (c) in KD patients. The proportions of $CD69^{+}$ cells were investigated in NK cells ($n = 35$), αβT cells ($n = 23$), γδT cells ($n = 23$) and B cells ($n = 35$). $^{**}P \leq 0{\cdot}0005$; $^{*}P \leq 0{\cdot}01$.

expression at acute phase of KD (median values: 4·5% at acute phase and 2·8% at convalescent phase).

## Microarray analysis of the gene expression in PBMCs from KD patients

*Pathway analysis.* To assess the innate and acquired immunological status in KD more precisely, the gene expression profiles of PBMCs from the patients were analysed by microarray. Six hundred and fifty-eight genes in PBMCs from KD patients showed more than twofold higher expression levels compared with those from healthy controls. These 658 genes were put into Pathway-Express in Onto-Tools (http://vortex.cs.wayne.edu). Pathway-Express searched the KEGG pathways in the Onto-Tools database for each input gene, and built a list of pathways [7]. Thirty-six pathways, associated significantly with acute phase of KD, were selected and the top 12 pathways are listed in Table 1. Among the pathways extracted by Pathway-Express, all input genes in antigen processing and presentation, T cell receptor (TCR)

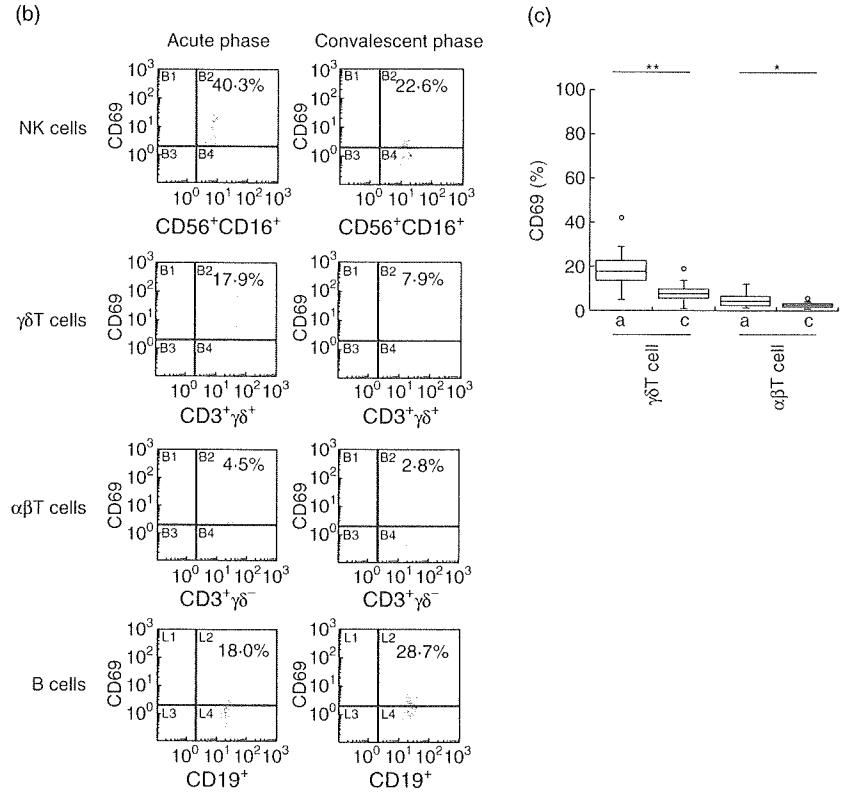


**Fig. 1.** *Continued*

**Table 1.** The results of the pathway impact analysis for a set of genes associated with acute phase of Kawasaki disease.

| Pathway name | Input genes in pathway | | | Impact factor | Corrected gamma *P*-value |
|---|---|---|---|---|---|
| | Total | Up | Down | | |
| Antigen processing and presentation | 7 | 0 | 7 | 51·621 | 2·01E-21 |
| Phosphatidylinositol signalling system | 2 | 0 | 2 | 35·807 | 1·04E-14 |
| Circadian rhythm | 3 | 0 | 3 | 22·942 | 2·60E-09 |
| T cell receptor signalling pathway | 14 | 0 | 14 | 18·903 | 1·23E-07 |
| Toll-like receptor signalling pathway | 14 | 6 | 8 | 18·526 | 1·76E-07 |
| Natural killer cell-mediated cytotoxicity | 14 | 4 | 10 | 14·664 | 6·71E-06 |
| Ribosome | 11 | 0 | 11 | 13·743 | 1·59E-05 |
| Apoptosis | 10 | 3 | 7 | 13·426 | 2·13E-05 |
| MAPK signalling pathway | 17 | 4 | 13 | 10·964 | 2·07E-04 |
| Cytokine–cytokine receptor interaction | 16 | 7 | 9 | 9·511 | 7·78E-04 |
| Fc epsilon RI signalling pathway | 8 | 3 | 5 | 9·323 | 9·22E-04 |
| B cell receptor signalling pathway | 7 | 0 | 7 | 8·690 | 0·00163044 |

Pathway-Express was used for the pathway impact analysis in order to build a list of all associated pathways. An impact factor (IF) is calculated for each pathway incorporating parameters such as the normalized fold change of the differentially expressed genes, the statistical significance of the set of pathway genes and the topology of the signalling pathway. The corrected gamma *P*-value is the *P*-value provided by the impact analysis. Thirty-six pathways were significant at the 5% level on corrected *P*-values, and the top 12 pathways were selected. Up-regulated genes were as follows: (i) Toll-like receptor signalling pathway; extracellular-regulated kinase (ERK), CD14, Toll-like receptor (TLR)-8, MAP kinase kinase 6 (MKK6), MD2 and TLR-5. (ii) Natural killer cell-mediated cytotoxicity; tumour necrosis factor-related apoptosis inducing ligand (TRAIL), ERK, Fc epsilon RI gamma (FCER1G) and TRAILR3. (iii) Apoptosis; TRAIL, protein kinase A regulatory subunit 1A (PRKAR1A) and TRAILR3. (iv) Mitogen-activated protein kinase (MAPK) signalling pathway; ERK, CD14, interleukin (IL)-1R2 and MKK6. (v) Cytokine–cytokine receptor interaction; TRAIL, tumour necrosis factor receptor superfamily, member 17 (TNF-RSF17), IL-18RAP, IL-1R2, TNF-SF13B, TRAILR3, and hepatocyte growth factor (HGF). (vi) Fc epsilon RI signalling pathway; ERK, FCER1G, and MKK6.

**Table 2.** Microarray analysis of peripheral blood mononuclear cells (PBMCs) between Kawasaki disease (KD) patients and healthy controls.

| Gene name | Gene ontology | Synonyms | GenBank | Fold difference* |
|---|---|---|---|---|
| NLR family, apoptosis inhibitory protein | Nucleotide binding | NAIP | NM_004536 | 7·2 |
| Fc fragment of IgG, high-affinity Ia, receptor (CD64) | Immune response | FCGR1A | NM_000566 | 5·6 |
| Haemoglobin, gamma A | Oxygen transport | HBG1 | NM_000559 | 5·3 |
| Haemoglobin, alpha 1 | Oxygen transport | HBA1 | NM_000558 | 5·1 |
| Grancalcin, EF-hand calcium-binding protein | Calcium ion binding | GCA | NM_012198 | 4·5 |
| Fibrinogen-like 2 (constitutively expressed in cytotoxic T-cells) | Signal transduction | FGL2 | NM_006682 | 4·4 |
| Ice protease-activating factor | Defence response to bacterium | NLRC4 (IPAF) | NM_021209 | 4·2 |
| Placenta-specific 8 | | PLAC8 | NM_016619 | 4·1 |
| Immunoglobulin superfamily, member 6 | Immune response | IGSF6 | NM_005849 | 4·1 |
| S100 calcium binding protein A9 (calgranulin B) | Inflammatory response | S100A9 | NM_002965 | 3·9 |

*The difference of mean gene expression levels between 3 KD patients and controls (healthy donors) in microarray analysis is given. NLR: nucleotide-binding domain, leucine-rich repeat containing. Genes that showed more than threefold expressional differences between KD patients and healthy controls were selected and the top 10 genes were listed. Gene ontology was not applied in PLAC8. Hypothetical proteins were excluded. IgG: immunoglobulin G; EF hand: The EF-hand describes the nearly perpendicular arrangement of the E and F helices flanking the 12-residue $Ca^{2+}$-binding loop, in analogy to the stretched out right hand with the forefinger (E helix) and thumb (F helix) and the remaining fingers folded to form the $Ca^{2+}$-binding loop.

signalling pathway and B cell receptor (BCR) signalling pathway, which are involved in acquired immunity, were down-regulated. Conversely, TLR signalling and NK cell-mediated cytotoxicity pathways, related closely to innate immunity, were partly up-regulated.

*Top 10 genes in microarray analysis.* In microarray analysis, 47 genes in KD patients were up-regulated more than threefold compared with those in healthy controls, and the top 10 genes are shown in Table 2. Among them, five genes such as nod-like receptor (NLR) family, apoptosis inhibitory protein (NAIP), NLRC4 (IPAF), S100A9 protein, Fc fragment of IgG, high-affinity Ia, receptor (FCGR1A, also known as CD64) and grancalcin (GCA, EF-hand calcium-binding protein) were related closely to innate immune responses [13–17], while three genes such as fibrinogen-like protein 2 (FGL2), placenta-specific 8 (PLAC8) and immunoglobulin superfamily, member 6 (IGSF6) were related to both innate and acquired immunity [18–20].

## Cytokine analyses in KD patients

*Microarray analysis.* Sixteen genes that have been reported to have a role in the pathophysiology of KD were selected from the microarray data, and the relative gene expression levels in PBMCs of KD patients compared with those of healthy controls are shown in Table 3. Expression levels of *S100A9* and *S100A12* genes, which encode the

**Table 3.** Cykokine- and chemokine-related genes expressed in peripheral blood mononuclear cells (PBMCs) of acute-phase Kawasaki disease (KD) patients.

| Gene name | Gene ontology | Synonyms | GenBank | Fold difference* |
|---|---|---|---|---|
| Interleukin 1 beta | Immune response | IL-1B | NM_000576 | 0·3 |
| Interleukin 2 | Immune response | IL-2 | NM_000586 | 0·7 |
| Interleukin 4 | Regulation of immune response | IL-4 | NM_000589 | 0·4 |
| Interleukin 6 | Inflammatory response | IL-6 | NM_000600 | 0·5 |
| Interleukin 8 | Immune response | IL-8 | NM_000584 | 0·2 |
| Interleukin 10 | Immune response | IL-10 | NM_000572 | 0·8 |
| Tumour necrosis factor | Inflammatory response | TNF | NM_000594 | 0·9 |
| Interferon gamma | Regulation of immune response | IFN-γ | NM_000619 | 0·9 |
| Chemokine (C-C motif) ligand 2 | Inflammatory response | CCL2 (MCP1) | NM_002982 | 1·1 |
| Chemokine (C-C motif) ligand 4 | Immune response | CCL4 (MIP1B) | NM_002984 | 0·6 |
| Chemokine (C-C motif) ligand 5 | Immune response | CCL5 (RANTES) | NM_002985 | 0·4 |
| Colony stimulating factor 3 (granulocyte) | Immune response | CSF3 | NM_172220 | 1·0 |
| Vascular endothelial growth factor A | Cytokine activity | VEGFA | NM_001025366 | 0·4 |
| Hepatocyte growth factor | Protein binding | HGF | NM_000601 | 2·8 |
| S100 calcium binding protein A9 (calgranulin B) | Inflammatory response | S100A9 | NM_002965 | 3·9 |
| S100 calcium binding protein A12 | Inflammatory response | S100A12 | NM_005621 | 3·5 |

*The difference of mean gene expression levels between three KD patients and controls (healthy donors) in microarray analysis is given. Sixteen genes that have been reported to have a role in the pathophysiology of KD were selected from the microarray data.

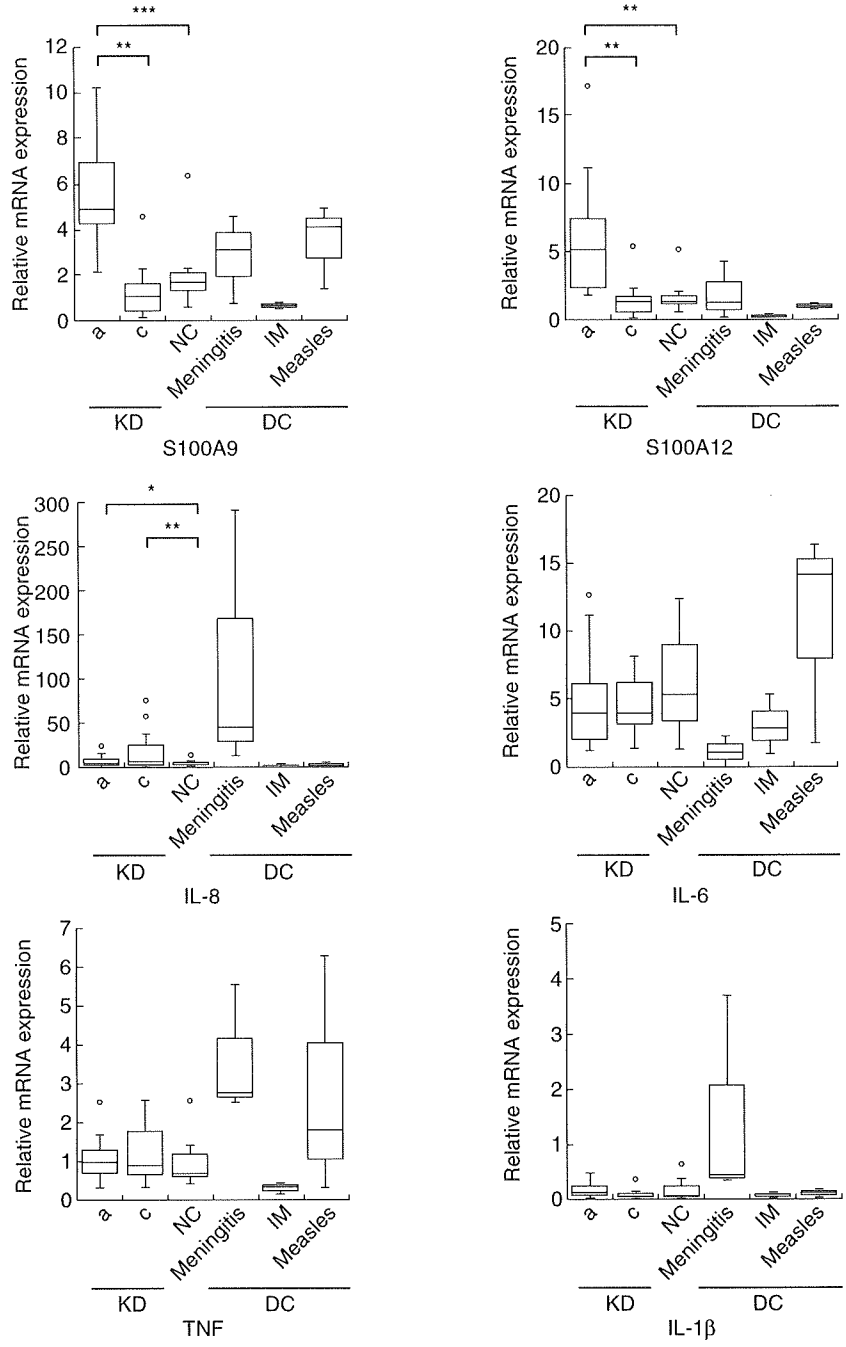


**Fig. 2.** Relative expression levels of *S100A9*, *S100A12*, *IL8*, *IL6*, *TNF* and *IL1B* genes in peripheral blood mononuclear cells (PBMCs) at acute phase of Kawasaki disease (KD). The gene expression levels of these cytokines were determined by the reverse transcription–polymerase chain reaction (RT–PCR) method using glyceraldehyde-3-phosphate-dehydrogenase (GAPDH) as an internal control. Gene expression levels of PBMCs from 10 KD patients, 11 healthy controls (NC), nine diseased control subjects [three patients with meningitis, three patients with acute infectious mononucleosis (IM) and three patients with measles] are shown. Only *IL8* gene expression levels were analysed in 16 KD patients. The form of box-plot was the same as Fig. 1. $^{*}P < 0{\cdot}05$; $^{**}P < 0{\cdot}01$; $^{***}P < 0{\cdot}001$. (a) Acute phase; (c) convalescent phase.

proinflammatory factors in innate immunity, as well as of the hepatocyte growth factor (*HGF*) gene, were more than twofold higher in KD patients than in healthy controls, while the expression levels of other cytokine, chemokine and growth factor genes were not elevated. Decreased gene expression levels of *IL4*, *IL10* and *IFNG* in KD patients were consistent with our previous data obtained by quantitative RT–PCR [21].

*Quantitative RT–PCR analysis.* To confirm the microarray data, the gene expression levels of six major cytokines, S100A9, S100A12, IL-8, IL-6, TNF-α and IL-1β, were analysed in KD patients and controls by quantitative RT–PCR. As shown in Fig. 2, the relative expression levels of *S100A9* and *S100A12* genes in PBMCs at acute-phase KD were significantly higher than those at convalescent-phase KD, consistent with previous reports [5,22]. Expression levels of the *IL8* gene at both acute and convalescent phases of KD were slightly but significantly higher than those of healthy controls. The expression levels of *TNF*, *IL1B* and *IL6* genes at either acute or convalescent phases of KD were not significantly different from those in healthy controls.

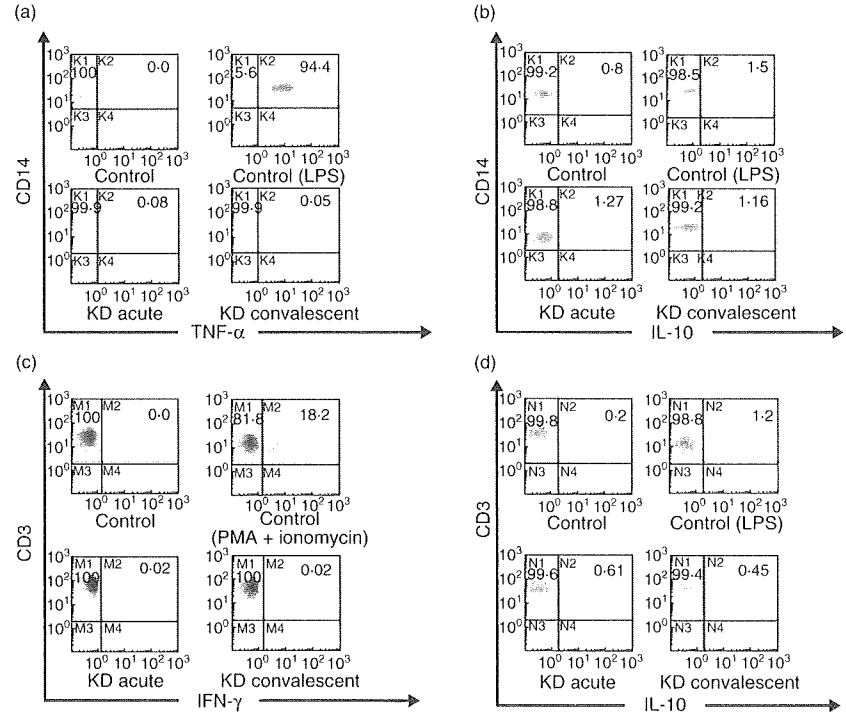


**Fig. 3.** Flow cytometric analysis of intracellular cytokine production of peripheral blood mononuclear cells (PBMCs) at acute phase of Kawasaki disease (KD). Intracellular cytokine production in PBMCs at acute and convalescent phases of KD was analysed by flow cytometry. Representative data of tumour necrosis factor (TNF)-α (a) and interleukin (IL)-10 (b) staining in monocytes, and those of interferon (IFN)-γ (c) and IL-10 (d) staining in T cells are shown. As positive and negative controls, representative data of TNF-α (a) and IL-10 (b) staining in monocytes with and without crude lipopolysaccharide (LPS) (1 μg/ml), and IFN-γ (c) and IL-10 (d) staining in T cells with and without phorbol 12-myristate 13-acetate (PMA) (25 ng/ml) plus ionomycin (1 μg/ml) are shown. The figure shows representative results of seven KD patients and three healthy controls.

*Intracellular cytokine analysis.* We analysed intracellular cytokines in the freshly isolated PBMCs at acute and convalescent phases of KD by using flow cytometry. Intracellular TNF-α or IL-10 production in monocytes and IFN-γ or IL-10 production in T cells were analysed in the peripheral blood of KD patients. As shown in Fig. 3, the percentages of both TNF-α or IL-10-producing cells in monocytes and IFN-γ or IL-10-producing cells in T cells were not significantly different between acute phase (TNF-α-producing cells: median 0·08%, range 0·04–0·09%; IL-10-producing cells: median 1·27%, range 0·47–1·31% in monocytes; IFN-γ-producing cells: median 0·02%, range 0·00–0·03%; IL-10–producing cells: median 0·61%, range 0·35–0·69% in T cells) and convalescent phase (TNF-α-producing cells: median 0·05%, range 0·00–0·08%; IL-10-producing cells: median 1·16%, range 0·79–2·43% in monocytes; IFN-γ-producing cells: median 0·02%, range 0·00–0·07%; IL-10-producing cells, median 0·45%, range 0·40–0·70% in T cells), further suggesting little intracellular production of such cytokines by peripheral blood cells at acute-phase KD.

## Discussion

Massive releases of cytokines, chemokines and growth factors play a pivotal role in the immunopathogenesis of KD [1]. Although numerous immunological studies on peripheral blood leucocytes have been reported, the status of peripheral T cell activation remains controversial [3]. In this regard, no previous studies have analysed T cells by separating them into two distinct populations, αβT cells and γδT cells, which are involved mainly in acquired and innate immunity, respectively. A predominant activation of γδT cells as well as NK cells in the present study, together with previous observations that neutrophils and monocytes are activated in KD [3,23,24], has suggested that innate immunity is involved actively in acute-phase KD. Although a recent report has shown no expansion of $CD69^+CD4^+$ or $CD69^+CD8^+$ cells in the peripheral blood of KD [25], it might have been difficult to detect the increases of $CD69^+$ T cells in the peripheral blood without the separation into αβ and γδT cells, because a major $CD69^+$ T cell population resided in $CD4^-CD8^{-/dim+}$ γδT cells in KD.

In KD, it has been thought that most activated T cells moved to local tissues from peripheral blood at acute phase and returned from there at convalescent phase [3]. However, because significant proportions of activated γδT cells and NK cells with a small proportion of activated αβT cells were detected constantly in the peripheral blood at acute-phase KD, we performed DNA microarray analysis of PBMCs to check the activation status of these cells. Pathway analysis revealed that the pathways involved in acquired immunity such as antigen processing and presentation, TCR signalling and BCR signalling were all down-regulated, and that innate immunity pathways such as TLR signalling and NK cell-mediated cytotoxicity were partly activated, with a large part of them down-regulated. These findings suggested that a small proportion of αβT cells and a considerable proportion of γδT cells were activated not through TCR signalling pathway by either conventional antigen or superantigen but directly through innate immunity receptors and/or cytokine signalling pathways.

Among the top 10 genes whose expression was more than threefold higher in KD than in normal controls, five genes were related to innate immunity and two of the five were molecules associated with the NLR signalling pathway. Popper *et al.* reported that the expression levels of genes involved in innate immunity, proinflammatory responses and neutrophil activation and apoptosis were up-regulated and those related to NK cells and $CD8^+$ lymphocytes were down-regulated at acute-phase KD by DNA microarray analysis of peripheral whole blood cells, including neutrophils [26]. Verma *et al.* have also reported the up-regulated expression of the genes related to innate immunity such as the TLR signalling pathway, complement activation and matrix-adhesion molecule at acute-phase KD [27]. These studies demonstrated consistently the importance of innate immunity in the pathophysiology of acute-phase KD.

Although monocytes in the peripheral blood are considered to be activated *in vivo* in KD [3], there have been few reports showing that monocytes are actually producing such cytokines as IL-6, IL-8 and TNF *in vivo*, which are elevated in sera of KD patients. Abe *et al.* [5] demonstrated that there were no significant differences in the expression levels of *IL6*, *IL8* and *TNF* genes in separated monocytes before and after high-dose gammaglobulin therapy. Rather, monocytes are actively producing unique cytokines such as damage-associated molecular pattern molecules (DAMPs) (S100A9, S100A12) [5], one of which was reported to be produced by monocytes through the interaction with TNF-activated endothelial cells [14]. In our study, no significant differences of *IL6*, *IL1B* or *TNFA* mRNA levels in PBMCs were detected among patients with acute-phase KD, those with convalescent-phase KD and controls by microarray and quantitative RT–PCR. In the *IL8* gene expression, however, quantitative RT–PCR analysis of samples from a larger number of patients showed that slightly increased expression levels of the *IL8* gene at both acute and convalescent phases of KD, suggesting a weak activation of monocytes among PBMC. Although a previous study showed that 1–2% of PBMCs were positive for intracellular IL-6, TNF-$\alpha$ or TNF-$\beta$ by immunofluorescent microscopy [28], our analysis of blood samples shortly after drawing revealed no expansion of intracellular TNF-$\alpha$, IL-10 or IFN-$\gamma$-positive cells in acute-phase KD by flow cytometry.

We confirmed that the inositol 1, 4, 5-trisphosphate 3-kinase C (ITPKC) gene was associated with the development of KD [29] in our KD samples (data not shown), but presumably ITPKC acts mainly as a regulator of innate immune cells or non-immune cells (endothelial cells) rather than of $\alpha\beta$T cells, because (i) only a small fraction of $\alpha\beta$T cells showed an activation marker *in vivo*; (ii) the pathways involved in acquired immunity were all down-regulated (Table 1); and (iii) we have found a significant association between an innate immunity receptor gene and KD development, and have established a new KD mouse model with coronary arteritis by an innate immunity receptor ligand (unpublished observations).

In conclusion, the present data have indicated that PBMC showed a unique activation status with high expression of DAMP genes but low expression of proinflammatory cytokine genes, and that the innate immune system appears to play a role in the pathogenesis and pathophysiology of KD. Further studies are needed to elucidate the mechanism responsible for the development of KD and coronary arteritis in terms of the activation of the innate immune system both *in vitro* and *in vivo*.

## Acknowledgements

This work was supported by Ministry of Health, Labour and Welfare (MHLW), Health and Labour Sciences Research Grants, Comprehensive Research on Practical Application of Medical Technology: Randomized Controlled Trial to Assess Immunoglobulin plus Steroid Efficacy for Kawasaki Disease (RAISE) Study (grant 008), a grant-in-aid for scientific research from the Ministry of Education, Culture, Sports, Science, and Technology of Japan (grant 21790993), grants from the Japan Therapeutic Study Group for Kawasaki Disease (JSGK), and grants from the Japan Kawasaki Disease Research Center.

## Disclosure

None.

## References

1 Burns JC, Glode MP. Kawasaki syndrome. Lancet 2004; **364**:533–44.
2 Rowley AH, Baker SC, Orenstein JM, Shulman ST. Searching for the cause of Kawasaki disease – cytoplasmic inclusion bodies provide new insight. Nat Rev Microbiol 2008; **6**:394–401.
3 Matsubara T, Ichiyama T, Furukawa S. Immunological profile of peripheral blood lymphocytes and monocytes/macrophages in Kawasaki disease. Clin Exp Immunol 2005; **141**:381–7.
4 Ichiyama T, Yoshitomi T, Nishikawa M *et al.* NF-kappaB activation in peripheral blood monocytes/macrophages and T cells during acute Kawasaki disease. Clin Immunol 2001; **99**:373–7.
5 Abe J, Jibiki T, Noma S, Nakajima T, Saito H, Terai M. Gene expression profiling of the effect of high-dose intravenous Ig in patients with Kawasaki disease. J Immunol 2005; **174**:5837–45.
6 Akagi T, Rose V, Benson LN, Newman A, Freedom RM. Outcome of coronary artery aneurysms after Kawasaki disease. J Pediatr 1992; **121**:689–94.
7 Khatri P, Voichita C, Kattan K *et al.* Onto-Tools: new additions and improvements in 2006. Nucleic Acids Res 2007; **35**: W206–11.
8 Draghici S, Khatri P, Tarca AL *et al.* A systems biology approach for pathway level analysis. Genome Res 2007; **17**:1537–45.
9 Kanehisa M, Goto S, Kawashima S, Nakaya A. The KEGG databases at GenomeNet. Nucleic Acids Res 2002; **30**:42–6.
10 Furuno K, Yuge T, Kusuhara K *et al.* CD25+CD4+ regulatory T cells in patients with Kawasaki disease. J Pediatr 2004; **145**:385–90.

 

11 Monney L, Sabatos CA, Gaglia JL *et al.* Th1-specific cell surface protein Tim-3 regulates macrophage activation and severity of an autoimmune disease. Nature 2002; **415**:536–41.
12 Takada H, Yoshikawa H, Imaizumi M *et al.* Delayed separation of the umbilical cord in two siblings with interleukin-1 receptor-associated kinase 4 deficiency: rapid screening by flow cytometer. J Pediatr 2006; **148**:546–8.
13 Fritz JH, Ferrero RL, Philpott DJ, Girardin SE. Nod-like proteins in immunity, inflammation and disease. Nat Immunol 2006; **7**:1250–7.
14 Foell D, Wittkowski H, Vogl T, Roth J. S100 proteins expressed in phagocytes: a novel group of damage-associated molecular pattern molecules. J Leukoc Biol 2007; **81**:28–37.
15 Foell D, Wittkowski H, Roth J. Mechanisms of disease: a 'DAMP' view of inflammatory arthritis. Nat Clin Pract Rheumatol 2007; **3**:382–90.
16 Perussia B, Dayton ET, Lazarus R, Fanning V, Trinchieri G. Immune interferon induces the receptor for monomeric IgG1 on human monocytic and myeloid cells. J Exp Med 1983; **158**:1092–113.
17 Panelli MC, Wang E, Phan G *et al.* Gene-expression profiling of the response of peripheral blood mononuclear cells and melanoma metastases to systemic IL-2 administration. Genome Biol 2002; **3**:RESEARCH0035.
18 Chan CW, Kay LS, Khadaroo RG *et al.* Soluble fibrinogen-like protein 2/fibroleukin exhibits immunosuppressive properties: suppressing T cell proliferation and inhibiting maturation of bone marrow-derived dendritic cells. J Immunol 2003; **170**:4036–44.
19 Rissoan MC, Duhen T, Bridon JM *et al.* Subtractive hybridization reveals the expression of immunoglobulin-like transcript 7, Eph-B1, granzyme B, and 3 novel transcripts in human plasmacytoid dendritic cells. Blood 2002; **100**:3295–303.
20 King K, Moody A, Fisher SA *et al.* Genetic variation in the IGSF6 gene and lack of association with inflammatory bowel disease. Eur J Immunogenet 2003; **30**:187–90.
21 Kimura J, Takada H, Nomura A *et al.* Th1 and Th2 cytokine production is suppressed at the level of transcriptional regulation in Kawasaki disease. Clin Exp Immunol 2004; **137**:444–9.
22 Ebihara T, Endo R, Kikuta H *et al.* Differential gene expression of S100 protein family in leukocytes from patients with Kawasaki disease. Eur J Pediatr 2005; **164**:427–31.
23 Suzuki H, Noda E, Miyawaki M, Takeuchi T, Uemura S, Koike M. Serum levels of neutrophil activation cytokines in Kawasaki disease. Pediatr Int 2001; **43**:115–19.
24 Biezeveld MH, van Mierlo G, Lutter R *et al.* Sustained activation of neutrophils in the course of Kawasaki disease: an association with matrix metalloproteinases. Clin Exp Immunol 2005; **141**: 183–8.
25 Brogan PA, Shah V, Clarke LA, Dillon MJ, Klein N. T cell activation profiles in Kawasaki syndrome. Clin Exp Immunol 2008; **151**:267–74.
26 Popper SJ, Shimizu C, Shike H *et al.* Gene-expression patterns reveal underlying biological processes in Kawasaki disease. Genome Biol 2007; **8**:R261.
27 Verma S, Melish ME, Volper E *et al.* Analysis of disease-associated genes and proteins in Kawasaki disease. Abstracts of the 9th International Kawasaki Disease Symposium 2008:44.
28 Eberhard BA, Andersson U, Laxer RM, Rose V, Silverman ED. Evaluation of the cytokine response in Kawasaki disease. Pediatr Infect Dis J 1995; **14**:199–203.
29 Onouchi Y, Gunji T, Burns JC *et al.* ITPKC functional polymorphism associated with Kawasaki disease susceptibility and formation of coronary artery aneurysms. Nat Genet 2008; **40**:35–42.

Mod Rheumatol
DOI 10.1007/s10165-009-0249-y

CASE REPORT

# A case of familial Mediterranean fever associated with compound heterozygosity for the pyrin variant L110P-E148Q/M680I in Japan

**Koichi Oshima · Kazuko Yamazaki · Yoichi Nakajima · Akari Kobayashi · Tomochika Kato · Osamu Ohara · Kazunaga Agematsu**

Received: 18 August 2009 / Accepted: 23 October 2009


**Abstract** Familial Mediterranean fever (FMF) is an autosomal recessive disorder characterized by recurrent and self-limited fever attacks and serositis/arthritis. The M694V, M694I, M680I, V726A, and E148Q mutations in *MEFV*, the gene responsible for FMF, account for most FMF cases in Mediterranean populations. In Japan, M694I and E148Q are most frequently detected; M694V, M680I, and V726A have not been identified so far. We report the first case of FMF associated with M680I in Japan.

**Keywords** Familial Mediterranean fever · M680I · MEFV

## Introduction

Familial Mediterranean fever (FMF) is an autosomal recessive disorder that is particularly common in Mediterranean populations [1]. It is characterized by recurrent and self-limited attacks of fever, serositis or arthritis and subsequent secondary amyloidosis [1–3]. The gene responsible for FMF-the Mediterranean fever gene (*MEFV*)-has been mapped to chromosome 16p13.3 [4–6]. It consists of 10 exons and encodes a protein comprising 781 amino acids called pyrin or marenostrin, which is expressed mainly in granulocytes and monocytes [4, 5]. So far, 184 mutations and polymorphisms of this gene have been identified [7]. Five common mutations (M694V, M694I, M680I, V726A, and E148Q) account for the vast majority of FMF mutations [8–10]. The clinical symptoms of FMF vary according to the mutations of *MEFV*. The M694V homozygote and compound heterozygote for M694V are associated with greater disease severity [11, 12]. Notably, E148Q is found in 16–25% of normal individuals in Japan [13], and it is known that compound heterozygous mutations of E148Q with M694V, M694I, M680I or V726A cause FMF.

In Japanese individuals, FMF is an extremely rare disease because of the low allele frequencies of the disease-causing mutations [13]. E148Q/M694I seem to be the most frequent alleles in Japanese FMF patients [13–15]. The M694V, M680I, and V726A mutations have not been found in Japan so far; herein, we report the first case in Japan of FMF in a patient who is compound heterozygote for L110P–E148Q/M680I.

## Case report

A 7-year-old Japanese boy was brought to our hospital in 2007 for periodic fever accompanied by chest pain. He had experienced fever and chest pain once a year since the age of 3 years. The fever and chest pain continued for about 3 days after onset, and then disappeared spontaneously.

K. Oshima (✉) · O. Ohara
Laboratory for Immunogenomics, Research Center for Allergy and Immunology, RIKEN, Yokohama Institute, Yokohama, Japan
e-mail: oshima-k@umin.ac.jp

K. Yamazaki · K. Agematsu
Department of Infection and Host Defense, Shinshu University Graduate School of Medicine, Shinshu University School of Medicine, Matsumoto, Japan

Y. Nakajima · A. Kobayashi · T. Kato
Department of Pediatrics, Toyokawa City Hospital, Toyokawa, Japan

O. Ohara
Department of Human Genome Technology, Kazusa DNA Research Institute, Kisarazu, Japan

Published online: 08 December 2009